ISSN 1849–0751 (On–line)
ISSN 0013–7448 (Print)
UDK 621.31

https://doi.org/10.37798/EN2022714

Journal of Energy

VOLUME 71 Number 4 | 2022

ENERGIJA 71

Journal of Energy

Scientific Professional Journal Of Energy, Electricity, Power Systems
Online ISSN 1849–0751, Print ISSN 0013–7448, VOL 71
https://doi.org/10.37798/EN2022714

Published by
HEP d.d., Ulica grada Vukovara 37, HR–10000 Zagreb
HRO CIGRÉ, Berislavićeva 6, HR–10000 Zagreb

EDITORIAL

The first paper is “Use of Supporting Software Tool for Decision-Making During Low-Probability Severe Accident Management at Nuclear Power Plants”. The NARSIS project focused on enhancing the safety assessment of nuclear power plants, including the management of low probability accident scenarios. As part of this project, a software tool called Severa was developed to support decision-making during severe accidents and describe in this paper. Severa interprets and monitors key physical measurements, assesses the state of critical barriers, predicts accident progression without intervention, and provides a list of recovery strategies and courses of action. The tool evaluates the feasibility and consequences of each action course, ranks them, and offers recommendations to the technical support center (TSC). The verification and validation of Severa demonstrated its potential for accident management, although it is currently in a simplified state.

The second paper is “On Minimal Cut Sets Representation with Binary Decision Diagrams”. Binary Decision Diagrams (BDDs) have gained significant acceptance in various industrial applications since their introduction as a representation of logical functions. This paper focuses on summarizing the properties of BDD representations of Minimal Cut Sets (MCS) in Fault Tree (FT) models commonly found in the nuclear energy field. The paper highlights the algorithms used for conditional probability evaluation and cut set selection on BDDs, which are crucial for unbiased quantitative analysis and event importance determination. The compactness of BDD representations is evaluated on real-life models from the Nuclear Power Plant Krško, demonstrating its effectiveness in implementing dynamic analysis and facilitating software upgrades. The key advantage of BDD-based analysis is its compact representation and the ability to perform qualitative and quantitative analysis on complete MCS sets, irrespective of the number of cut sets in the MCS set.

The third paper is “The progression of Guarantees of Origin trading in Croatia amidst the European framework”. This article examines the development and progress of Guarantees of Origin (GO) trading in Croatia, with a focus on the regulatory framework established by the Republic of Croatia. The responsibility for issuing GO for electricity and managing the Registry of Guarantees of Origin lies with the Croatian Energy Market Operator (HROTE). The article also discusses the background and development of GO trading in Croatia, positioning the country as a leader in the European context. A comparative analysis with the Guarantees of Origin market in the United Kingdom is provided, considering the impact of Brexit on GO markets. The article further explores the segregation of GO auctions based on specific technologies and characteristics of power plants, resulting in varying prices depending on the plant’s age or installed capacity.

The fourth paper is “Corrosion Detection and Surface Repair with Coatings on Condensate Storage Tanks Internal Surfaces”. The paper deals with the Nuclear power plant Krško. There are two single-hull condensate storage tanks with floating diaphragms that hold up to 757 m3 of demineralized water. These tanks play a crucial role in providing cooling water for the reactor coolant system and are classified as safety class 3 components. During the 2018 outage, the tanks were emptied and subjected to non-destructive examination (NDE) methods such as Magnetic Flux Leakage, Ultrasonic, and Vacuum Box inspections to identify corrosion damage and leaks in the floor plates and adjacent welds. The article discusses the NDE methods used, the process of internal surface repair with coatings, and the qualification of coatings for safety-related use. Extensive immersion tests were conducted to select the most suitable coating system.

The last paper is “Characterization of the GBC-32 Fuel Assembly Source Terms”. The paper presents selected results of TRITON-NEWT and TRITON depletion simulations of the OFA model in the framework of GBC-32 cask benchmark. This first phase is addressing accurate source terms characterization, since OFA model contains small modifications compared to the standard Westinghouse 17x17 FA model. Calculation of isotopic concentrations, decay heat, neutron-gamma spectra and major actinides activity for different fuel assembly cooling periods was performed using ORIGEN-ARP module. Besides quantification of neutron-gamma source terms, during burnup and cooling time periods, this methodology provides ability to generate cross-section database for each depleted material as a function of burnup in ORIGEN-S format.

Igor Kuzle
Editor–in–Chief

Journal of Energy

VOLUME 71 Number 4 | 2022

journal homepage: http://journalofenergy.com/

Use of Supporting Software Tool for Decision-Making During Low-Probability Severe Accident Management at Nuclear Power Plants

Luka Štrubelj[1], Klemen Debelak, Marko Bohanec, Adem Kikaj, Ivan Vrbanić, Ivica Bašić

***Summary* — In the project NARSIS – New Approach to Reactor Safety ImprovementS – possible advances in safety assessment of nuclear power plants (NPPs) were considered, which also included possible improvements in the field of management of low probability accident scenarios. As a part of it, a supporting software tool for making decisions under severe accident management was developed. The mentioned tool, named Severa, is a prototype demonstration-level decision supporting system, aimed for the use by the technical support center (TSC) while managing a severe accident, or for the training purposes. Severa interprets, stores and monitors key physical measurements during accident sequence progression. It assesses the current state of physical barriers: core, reactor coolant system, reactor pressure vessel and containment. The tool gives predictions regarding accident progression in the case that no action is taken by the TSC. It provides a list of possible recovery strategies and courses of action. The applicability and feasibility of possible action courses in the given situation are addressed. For each action course, Severa assesses consequences in terms of probability of the containment failure and estimated time window for failure. At the end, Severa evaluates and ranks the feasible actions, providing recommendations for the TSC. The verification and validation of Severa has been performed in the project and is also described in this paper. Although largely simplified in its current state, Severa successfully demonstrated its potential for supporting accident management and pointed toward the next steps needed with regard to further advancements in this field.**

***Keywords* — Severe accident management at NPP, decision supporting tool, decision model, technical support center**

(Corresponding author: Luka Štrubelj)

Luka Štrubelj and Klemen Debelak are with the GEN energija Krško, Slovenia (e-mails: luka.strubelj@gen-energija.si, klemen.debelak@gen-energija.si)

Marko Bohanec is with the Jožef Stefan Institute Ljubljana, Slovenia (e-mail: marko.bohanec@ijs.si)

Adem Kikaj is with the International Postgraduate School Jožef Stefan Ljubljana, Slovenia (e-mail: ademkikaj95@gmail.com)

Ivan Vrbanić and Ivica Bašić are with the APOSS Ltd Zabok, Croatia (e-mails: Ivan.vrbanic@zg.t-com.hr, basic.ivica@kr.t-com.hr)

[1] Statements expressed in the paper are author's own opinions, they are not binding for the company/institution in which author is employed nor they necessarily coincide with the official company/institution's positions.

1. Introduction

Academic, research and industrial European institutions from Slovenia (GEN, JSI), Croatia (APOSS), Italy (ENEA, UNIPI), France (CEA, BRGM, IRSN, EDF, Framatome – ex Areva NP), Austria (NUCCON), Poland (NCBJ, WUT), Germany (KIT, Framatome - ex. Areva), Finland (VTT), The Netherlands (TU Delft, NRG) and United Kingdom (EDF Energy) collaborated on the project NARSIS – New Approach to Reactor Safety ImprovementS [1]. The project was funded by the European Commission for the period of 4,5 years.

Based on recent theoretical progresses, the NARSIS project aimed at making significant scientific step forward towards addressing the update of some elements required for the safety assessment of NPPs. These improvements mainly concerned:

- Natural hazards characterization, in particular by considering concomitant external events, either simultaneous-yet-independent hazards or cascading events, and the correlation in intra-event intensity parameters.
- Vulnerability of the elements to complex aggressions, with the integration of new approaches such as vector-based fragility surfaces and reduced models
- Better treatment of uncertainties through adoption of probabilistic framework for vulnerability curves and non-probabilistic approach to constraining the "expert judgments".

The effectiveness of these improvements were tested and validated in the frame of the project through a set of laboratory experimentations and numerical simulations using generic nuclear power plant and real case applications.

The project was structured into seven work packages (WP):

- WP1: External hazards characterization,
- WP2: Fragility assessment of main NPPs critical elements,
- WP3: Integration and safety analysis,
- WP4: Applying and comparing various safety assessment approaches on a virtual reactor,
- WP5: Supporting tool for severe accident management,
- WP6: Dissemination, recommendation, and training,
- WP7: Project management and coordination.

The main goal of work package (WP5) was the development

Luka Štrubelj, Klemen Debelak, Marko Bohanec, Adem Kikaj, Ivan Vrbanić, Ivica Bašić, Use of Supporting Software Tool for Decision-Making During Low-Probability Severe Accident Management at Nuclear Power Plants, Journal of Energy, vol. 71 Number 4 (2022), 3–11
https://doi.org/10.37798/2022714423

of decision support tool for severe accident management and its demonstration., The referential nuclear power plant (NPP) was established [1]. The referential NPP was based on operating fleet in the European Union. The safety systems, structures and components (SSC) of referential nuclear power plant include design basis safety SSC, safety SSC to mitigate severe accidents and mobile SSC ("flexible" or FLEX equipment). The design basis SSC includes high pressure injection, borated water accumulators, and low-pressure safety injections, to supply cooling water and mitigate loss of coolant accident. Emergency diesel generators and batteries are intended to supply energy for operation of pumps, valves and instrumentation and control. Emergency feed water pumps are intended for reactor core cooling. The safety valves are installed at reactor coolant system to decrease pressure below design value. The containment prevents releases to the environment and radioactive doses to the public. Alternative energy sources in terms of diesel generators and batteries are included in the referential NPP.

Severe accident management guidelines (SAMGs) applicable to referential NPP were described [2]. In the case of deviation of important NPP measurements, alarms go off in the control room and the operators use alarm respond procedures to respond to alarms. In the case of unsuccessful correction of the situation, they use abnormal operating procedures. If the problems still persist and reactor trip is activated, it means that design basis accident is occurring and emergency operating procedures are used to activate safety SSC. If such action is not successful, the core starts to heat up due to decay heat and severe accident with core degradation or melting can occur. The management of NPP is transferred from operators in control room to the technical support center (TSC). In order to manage severe accidents, the SAMGs are used by managers in TSC. The SAMGs include operations such as:

a) Injection to steam generator, to remove decay heat from reactor coolant system (the so-called high-level action HLA1).

b) Depressurization of reactor coolant system, to prevent high pressure melted corium ejection, which can damage containment and causes quick rise of containment pressure and hydrogen generation (HLA2).

c) Injection to reactor coolant system, which assures coolant water to reactor core to remove decay heat (HLA3).

d) Injection of water into containment, to reduce containment pressure and possible radioactive releases.

The SAMGs imply that the TSC needs to take decisions. There could be large amount of information, available only partially, or with high uncertainty. The TSC managers are under stress due to an extensive damage in the NPP, potential releases of radionuclides and time pressure. The decision support tool Severa, developed in the project and described in this paper, targets accident management stage and aims at supporting the managers to make appropriate decisions with prioritization of actions in a well-justified and timely manner.

II. Input Data

The hazard-induced damage states and specific accident progression event tree for demonstration purposes were developed [3]. This includes developing accident progression logic structure for postulated hazard damage states, where damaged SSC are identified.

For this purpose, two major severe accident sequences were evaluated: high pressure (HP) and low pressure (LP) sequence. Figure 1 provides an indication of the time scale for the major phenomena. The high pressure sequence starts with an initiating event like station black out (total loss of internal and external electricity power), or loss of ultimate heat sink, where decay heat removal is absent and the depressurization of reactor coolant system fails. The core temperature starts to rise and hydrogen production starts in contact of hot steam and cladding. The core starts to melt and can be ejected, if hot leg creep failure did not occur, to containment with reactor vessel failure at high pressure (High Pressure Melt Ejection (HPME)). The fast transfer of corium heat in containment (Direct Containment Heating (DCH)) threatens containment integrity.

The low pressure sequence starts with an initiating event like loss of coolant accident, where the water in reactor coolant system is lost, and there is no medium to remove decay heat. The containment pressure starts to increase with loss of coolant accident, which can threaten the integrity of containment. The core temperature starts to rise. The core starts to melt and reactor vessel fails at the bottom. The reactor cavity below the reactor pressure vessel can be flooded with water. Hot corium in contact with water can initiate steam explosions, which can threaten containment integrity. The molten corium interaction with concrete and water starts to produce hydrogen and carbon monoxide (CO), which both can form explosive mixture. Potential hydrogen and CO burn or explosion can threaten the integrity of containment.

Severe accident simulations were performed for each sequence, with different safety features available and different time of activation of safety features [4].

The assessment of decisions needed to be taken by technical support center was carried out and the main decisions were identified and characterized. Then, the attributes against which all decisions are evaluated in decision support process were considered. Those included the status of main barriers, fuel cladding, reactor coolant boundary and containment. Since the status of boundaries (e.g. fuel temperatures) cannot be measured or observed directly, the related measurable parameters need to be used for diagnosis. Those are discussed in the next section.

Figure 1 presents a simplified severe accident progression, important phenomenology effects for both scenarios (LP and HP) including the comparison of expected (predicted by severe accident simulations with MELCOR code) time windows of each accident phase [4].

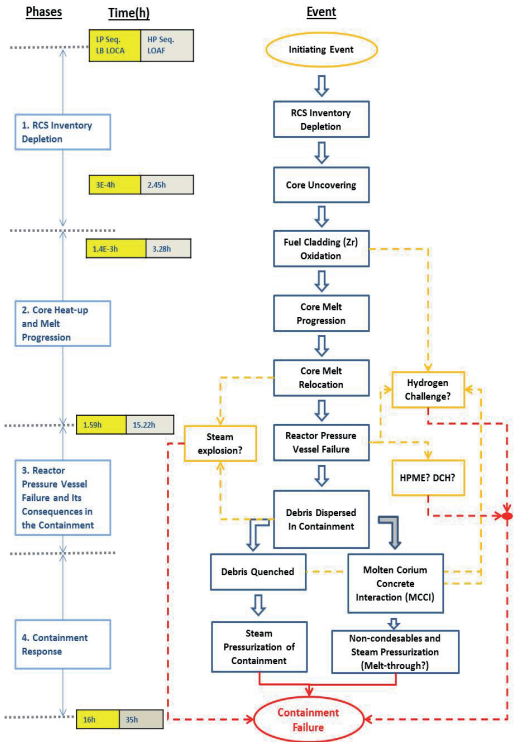

Fig. 1. Severe Accident Progression and Phenomenology

Luka Štrubelj, Klemen Debelak, Marko Bohanec, Adem Kikaj, Ivan Vrbanić, Ivica Bašić, Use of Supporting Software Tool for Decision-Making During Low-Probability Severe Accident Management at Nuclear Power Plants, Journal of Energy, vol. 71 Number 4 (2022), 3–11
https://doi.org/10.37798/2022714423

III. Decision Support Tool

The decision-support tool called Severa [5] is a demonstration-level Windows application, aimed at supporting the TSC team while managing a severe NPP accident.

Severa operates in 10–20-minute decision-support cycles that consist of the following steps:

1. Monitor the key NPP operating parameters and the availability and performance or plant systems.
2. Assess the damage state of the barriers. Identify barriers that are already challenged on may be challenged soon.
3. Predict possible future accident progressions and possible consequences in the case that no management actions are taken.
4. Identify possible alternatives (action courses); identified action courses include the actions which are required by the SAMGs (including the priorities given by the SAMGs) and consider the availability of plant systems/functions and time windows required for the implementation of each action.
5. For each identified alternative, assess its feasibility in the given situation.
6. Predict the possible consequences associated with each action course in terms of expected radioactive releases in the environment.
7. Compare the alternatives based on the expected releases and recommend the alternative to proceed with.
8. Implement the selected actions and observe plant's response.

Among these, the steps 1–7 are supported by Severa, mostly by carrying out the necessary simulations and calculations, and presenting the results in terms of (editable) tables, reports and charts to the users. Based on this information, the final step 8 is on behalf of the TSC team, who are also responsible for repeating the steps until the accident has been resolved.

Conceptually, the seven supported steps belong to two functional categories:

1. *Monitoring*: Observing and assessing the situation "as-is", without any human intervention. This category includes the steps 1–3.
2. *Management*: Supporting the decision-analysis and decision-support activities of the TSC, according to the steps 4–7. This encompasses the identification of possible management actions in a given situation and assessment of the possible consequences, including expected radioactive releases.

Another partial categorization of Severa's functionality can be made to:

1. *Diagnostics*: Assessing the current state of the NPP and its barriers (steps 1 and 2).
2. *Prognostics*: Predicting future events: accident progression (step 3), feasibility of actions (5) and their consequences (6).

The operation of Severa is based on a time series of eight critical parameters that are periodically measured in the NPP [7]:

- "CET": Core Exit Thermocouples [°C]
- "SGL": Steam Generator Level [m]
- "RPVL": Reactor Pressure Vessel Level [%]
- "Prcs": Reactor Coolant System Pressure [MPa]
- "Pcont": Containment Pressure [MPa]
- "Tcont": Containment Temperature [°C]
- "Lcont": Containment Water Level [m]
- "H2": Hydrogen concentration [%]

On this basis, Severa supports the monitoring steps 1–3 and makes a first major decision-support contribution by providing the following information to the TSC:

- Whether or not – and when – the conditions in the NPP require the activation of SAMGs?
- Which SAGs (Severe Accident Guidelines) are relevant for the situation? Currently, Severa is restricted to three SAGs: SAG-1 (Inject into SG), SAG-2 (Depressurization of Reactor Coolant System (RCS)) and/or SAG-3 (Inject into RCS).
- Given the measurements, what are the expected states of the three barriers: Core, RCS, and Containment?
- What are the expected progressions of the event if no actions are undertaken by the TSC?

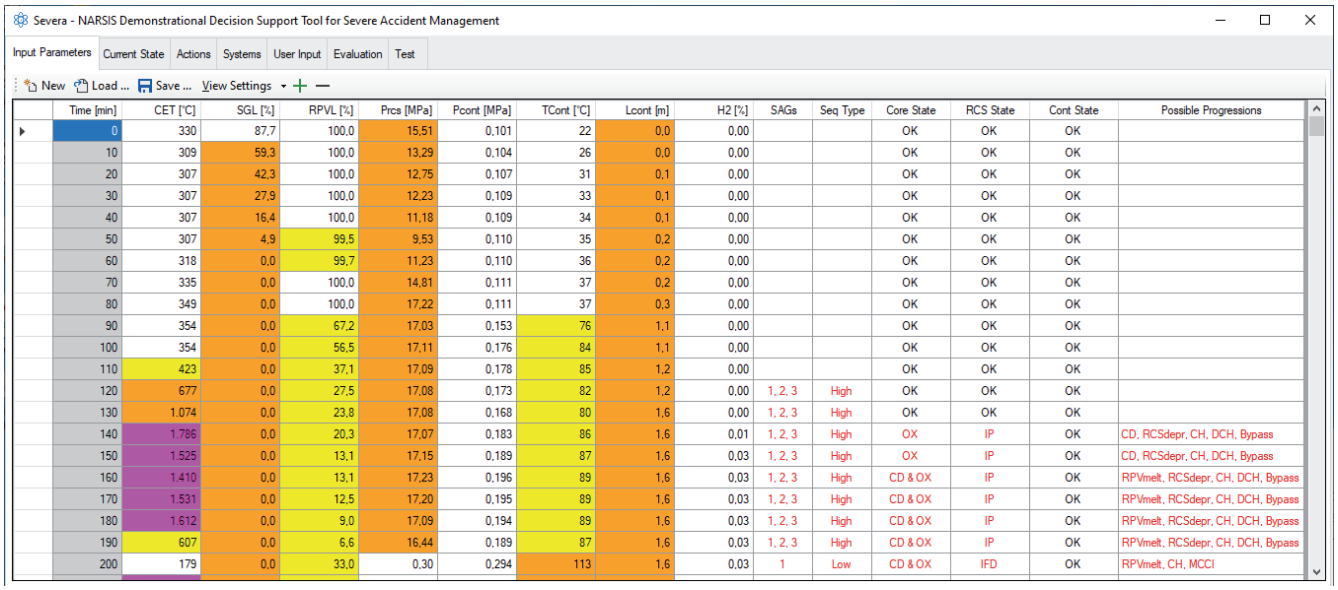

Time [min]	CET [°C]	SGL [%]	RPVL [%]	Prcs [MPa]	Pcont [MPa]	TCont [°C]	Lcont [m]	H2 [%]	SAGs	Seq Type	Core State	RCS State	Cont State	Possible Progressions
0	330	87,7	100,0	15,51	0,101	22	0,0	0,00			OK	OK	OK	
10	309	59,3	100,0	13,29	0,104	26	0,0	0,00			OK	OK	OK	
20	307	42,3	100,0	12,75	0,107	31	0,1	0,00			OK	OK	OK	
30	307	27,9	100,0	12,23	0,109	33	0,1	0,00			OK	OK	OK	
40	307	16,4	100,0	11,18	0,109	34	0,1	0,00			OK	OK	OK	
50	307	4,9	99,5	9,53	0,110	35	0,2	0,00			OK	OK	OK	
60	318	0,0	99,7	11,23	0,110	36	0,2	0,00			OK	OK	OK	
70	335	0,0	100,0	14,81	0,111	37	0,2	0,00			OK	OK	OK	
80	349	0,0	100,0	17,22	0,111	37	0,3	0,00			OK	OK	OK	
90	354	0,0	67,2	17,03	0,153	76	1,1	0,00			OK	OK	OK	
100	354	0,0	56,5	17,11	0,176	84	1,1	0,00			OK	OK	OK	
110	423	0,0	37,1	17,09	0,178	85	1,2	0,00			OK	OK	OK	
120	677	0,0	27,5	17,08	0,173	82	1,2	0,00	1, 2, 3	High	OK	OK	OK	
130	1.074	0,0	23,8	17,08	0,168	80	1,6	0,00	1, 2, 3	High	OK	OK	OK	
140	1.786	0,0	20,3	17,07	0,183	86	1,6	0,01	1, 2, 3	High	OX	IP	OK	CD, RCSdepr, CH, DCH, Bypass
150	1.525	0,0	13,1	17,15	0,189	87	1,6	0,03	1, 2, 3	High	OX	IP	OK	CD, RCSdepr, CH, DCH, Bypass
160	1.410	0,0	13,1	17,23	0,196	89	1,6	0,03	1, 2, 3	High	CD & OX	IP	OK	RPVmelt, RCSdepr, CH, DCH, Bypass
170	1.531	0,0	12,5	17,20	0,195	89	1,6	0,03	1, 2, 3	High	CD & OX	IP	OK	RPVmelt, RCSdepr, CH, DCH, Bypass
180	1.612	0,0	9,0	17,09	0,194	89	1,6	0,03	1, 2, 3	High	CD & OX	IP	OK	RPVmelt, RCSdepr, CH, DCH, Bypass
190	607	0,0	6,6	16,44	0,189	87	1,6	0,03	1, 2, 3	High	CD & OX	IP	OK	RPVmelt, RCSdepr, CH, DCH, Bypass
200	179	0,0	33,0	0,30	0,294	113	1,6	0,03	1	Low	CD & OX	IFD	OK	RPVmelt, CH, MCCI

Fig. 2. A Severa screenshot showing and interpreting the first 200 minutes of a Station Blackout scenario

Luka Štrubelj, Klemen Debelak, Marko Bohanec, Adem Kikaj, Ivan Vrbanić, Ivica Bašić, Use of Supporting Software Tool for Decision-Making During Low-Probability Severe Accident Management at Nuclear Power Plants, Journal of Energy, vol. 71 Number 4 (2022), 3–11
https://doi.org/10.37798/2022714423

Figure 2 shows an example of Severa screenshot that displays the first 200 minutes of a Station Blackout event (simulated with MELCOR) and Severa interpretation of the time series in terms of:

- Columns "CET" to "Lcont": Color-coded interpretation of individual measurements. White, yellow, orange and red colors indicate the states of increasing severity, and magenta indicates an out-of-range or erroneous measurements.
- Column "SAG": Shows SAGs relevant for the situation (multiple SAGs are possible).
- Column "Seq Type": Sequence type, either low-pressure or high-pressure.
- Columns "Core State" – "Cont State": Assessed current state of the three barriers. The acronyms represent cladding oxidation (OX), core damage (CD), intact pressurized (IP) and intact/failed depressurized (IFD).
- Column Possible Progressions: Prediction of possible events if no actions are undertaken.

This information is generated by Severa partly by using decision rules encoded in the software and partly by a qualitative rule-based multi-criteria model [9] developed according to the method DEX [8].

An important consequence of this approach is that each assessment, put forward by Severa, can be justified and explained in more detail when requested by the TSC. For example, Figure 3 shows a detailed description of the situation in the 120th minute of the Station Blackout scenario from Figure 2. The left-hand side shows the summary input parameter values at that time point, the set of entered SAGs, sequence type and a summary of barrier states. The right-hand side of Figure 3 displays detailed results of the evaluation carried out by the Barriers Progression DEX model. The report shows the hierarchical structure of attributes; for each individual attribute, it displays the qualitative value assigned to that attribute, which was determined from input sequence values and decision rules formulated in the model.

The second major decision-support contribution of Severa is related to possible management actions and their expected consequences (steps 4–7). In general decision-analysis terms, alternatives (or "decision alternatives") consist of multiple alternative courses of actions that may be undertaken in order to satisfy the decision makers' objectives. While managing a severe accident, the main objective is to mitigate the accident with minimum damage to the NPP and environment. In each situation, multiple actions may be available, but their choice and potential success depend of a variety of factors: preconditions for carrying out an action, current and expected future availability of equipment, available time window, action adequacy, etc. Actions may be mutually exclusive and the success of some action may depend of the success of another ones. In Severa, the possible actions with the availability of equipment are used to define alternatives.

Each action has a success window, defined using the 95th and 5th percentile of success times. The expected action success probability is estimated by cumulative lognormal distribution depending on T05 and T95 (Figure 4). Here, the lognormal distribution was selected because of its convenience and because it is often used for phenomenological probability quantifications in the Level 2 PSAs. Any other probability distribution or probability model may be used in future versions, based on the human reliability or human factor analyses.

In Severa, the expected outcome of actions is assessed using a probability distribution of expected radioactive releases with respect to four categories of radioactivity release [7]:

- RC-E: Containment failure with a significant release of radioactivity is expected within several hours.

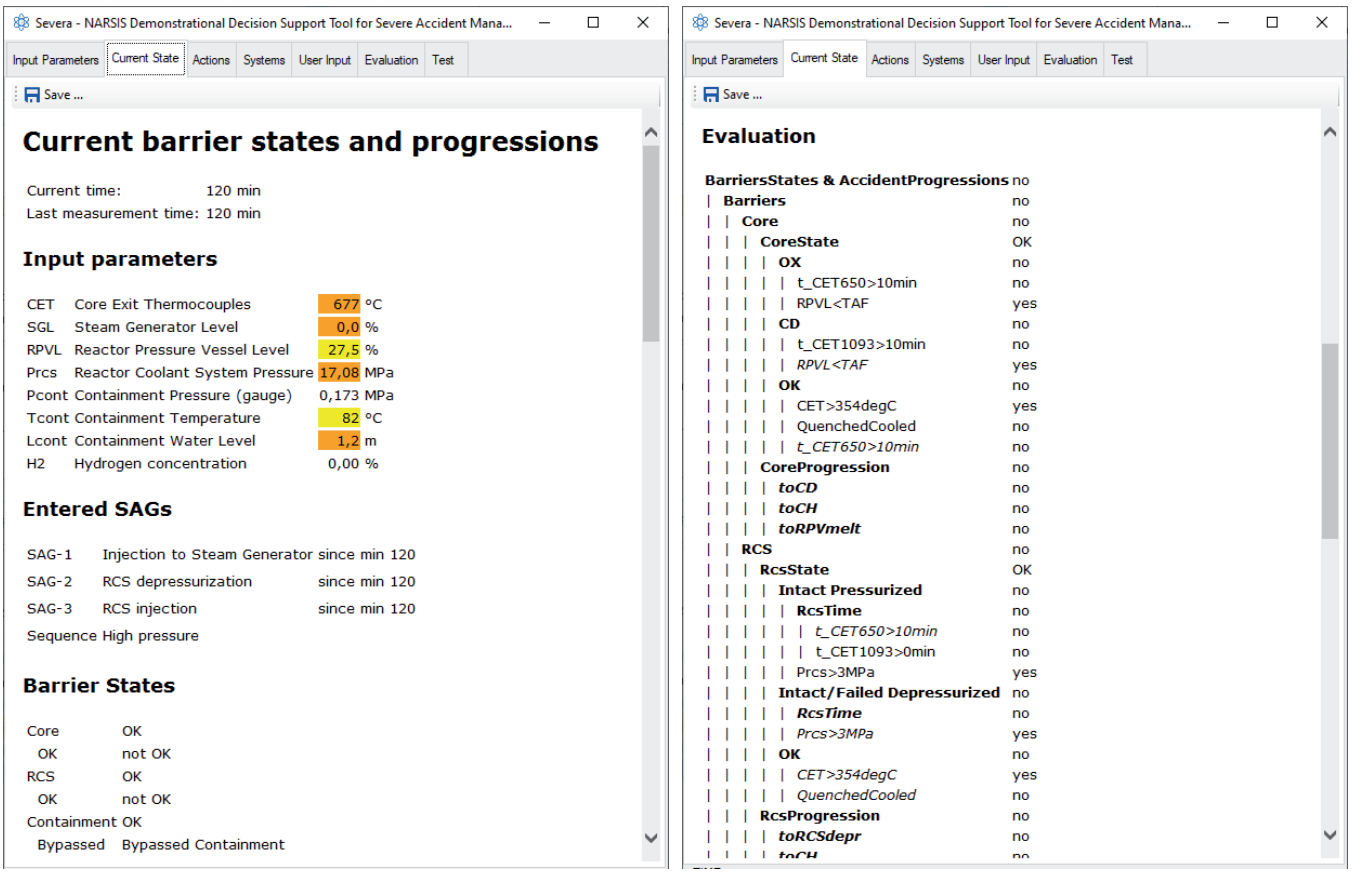

Fig. 3: The Current State report for minute 120 of Station Blackout

Luka Štrubelj, Klemen Debelak, Marko Bohanec, Adem Kikaj, Ivan Vrbanić, Ivica Bašić, Use of Supporting Software Tool for Decision-Making During Low-Probability Severe Accident Management at Nuclear Power Plants, Journal of Energy, vol. 71 Number 4 (2022), 3–11
https://doi.org/10.37798/2022714423

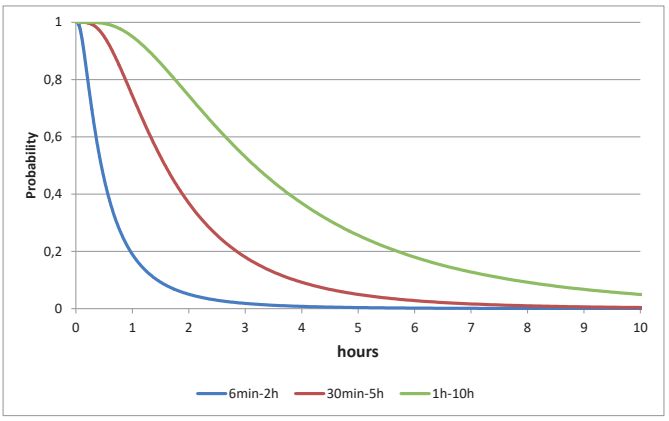

Fig. 4. Management actions' success windows in Severa

- RC-I: Containment failure with a significant release of radioactivity is expected within several days.
- RC-L: No significant release of radioactivity is expected within several days.
- RC-N: Long-term concern (in-vessel recovery and/or intact containment).

The main model for producing such assessments is based on an accident progression event tree (APET) [3], [4]. In Severa, the APET is implemented in terms of an equivalent probabilistic DEX model [7].

Let us illustrate the above concepts on an example of two hypothetical alternatives available to the TSC team in the 120th minute of station blackout (Figure 5). Acronyms in the figure denote plant systems that can generally be used to mitigate the situation. For instance, AFW denotes Auxiliary Feedwater Pump, SGPORV SG Power-Operated Relief Valve, etc. The abbreviation "DEC" refers to "Design Extension Condition". In most cases it is here used with a reference to the systems or equipment provided to cope with DEC conditions. Colors in Figure 5 denote the availability of those systems. The prevailing color is red, indicating that the corresponding systems are damaged beyond repair or otherwise unavailable. Only a few systems are available (green) or expected to be available (activated or repaired) in the future (orange).

Fig. 5. Definition of two alternatives in Severa

The two alternatives, available to the TSC team in minute 120, are:

- *Alternative D* (for "Design-based", Figure 4, left): The use of adequate design-based equipment (SGPORV and DECSG) will be possible only after extensive reparation work that will take about 30 minutes.
- *Alternative F:* (for "Flexible", Figure 4, right): Using less adequate flexible equipment (DECSGPORV, FLEXSG) that can be set up in 10 minutes.

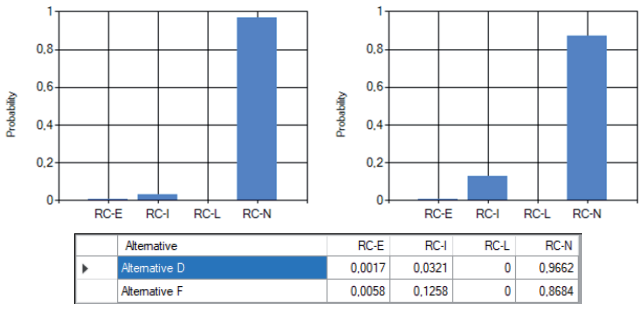

Alternative	RC-E	RC-I	RC-L	RC-N
Alternative D	0,0017	0,0321	0	0,9662
Alternative F	0,0058	0,1258	0	0,8684

Fig. 6. Probability distributions of radioactive releases for Alternatives D (left) and F (right)

Figure 6 shows the Severa's assessment of these alternatives in terms of probability distributions of RC-E, RC-I, RC-L and RC-N. Generally, when choosing between alternative actions, the action whose probabilities are the highest around RC-N and the lowest around RC-E is recommended for implementation. In this respect, Alternative D appears better than Alternative F, as its RC-N probability is considerably higher (0.9662 vs. 0.8684), while RC-E and RC-I are lower (0.0017 vs. 0,0058 and 0,0321 vs. 0.1258, respectively). Consequently, the TSC would be expected to choose Alternative D, initiate appropriate actions, and continue managing the accident carrying out next decision-making cycles.

It needs to be pointed out that Severa is a proof-of-concept tool which was developed in order to investigate the feasibility of this kind of decision support in severe accident management, primarily for the training purposes. As any such tool, it has its limitations. Among the most important is a treatment of time dependency of the probabilistic parameters incorporated in its prognostic logic. A number of phenomenological probabilities are presented by values which apply at an early phase of the accident and, therefore, its accurate performance is limited to this time window. Due to the complexity of the process, Severa relies on a simplified representation of its logic models, as well as a simplified consideration of adequacy of equipment included in the model and feedback from the implemented actions. At this point, Severa reflects three SAGs: SAG-1 (Inject into SG), SAG-2 (Depressurization of RCS) and/

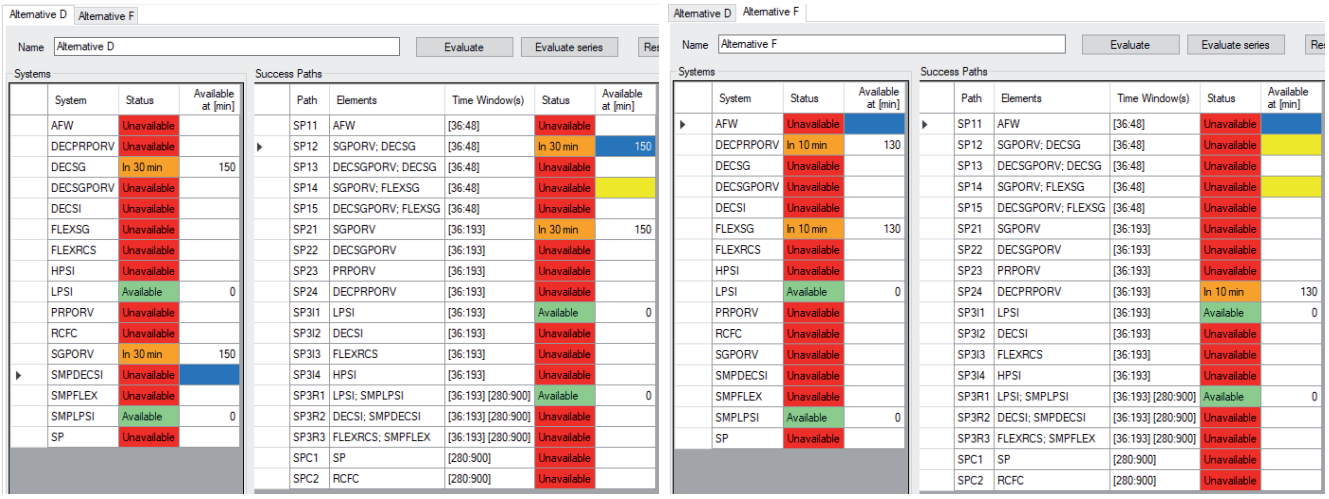

- *Alternative D* (for "Design-based", Figure 4, left): The

Luka Štrubelj, Klemen Debelak, Marko Bohanec, Adem Kikaj, Ivan Vrbanić, Ivica Bašić, Use of Supporting Software Tool for Decision-Making During Low-Probability Severe Accident Management at Nuclear Power Plants, Journal of Energy, vol. 71 Number 4 (2022), 3–11
https://doi.org/10.37798/2022714423

or SAG-3 (Inject into RCS). However, even under the limitations, the development of Severa was very challenging and took quite a considerable decision-analysis, decision-modelling and programming efforts. Verification and validation exercises showed that it can provide reasonable predictions of probability profiles of major release categories for the scenarios considered.

IV. Verification & Validation Of Severa

A. Basic definitions

Two terms are essential for Severa verification and validation (V&V) process. They are "Time Delay" and "Alternative". These two terms have a specific meaning in the context of Severa [9].

"*Time Delay*" is a user-provided input concerning the availability of critical systems / equipment. In Severa's prognostic model the availability of particular systems and their combinations is defined in terms of a "time delay" (TD), i.e., the time at which the respective item is expected to become available, measured from the time-point at which the assessment by Severa is being made. Following are some important points, with regard to V&V process:

- There are a certain number of TD terms for which values need to be entered by a user. Some of the terms relate to particular single systems, the others to combinations of systems. Those systems or their combinations comprise different possible "success paths" via which considered critical safety functions may be established / recovered.
- Generally, the designator "TDx" represents the time (starting from now ("now" meaning the time-point at which Severa is used)) at which system "x" would become available;
- It is noted that: $0 < TDx < \infty$:
  - $0 \rightarrow$The value "0" means that system (item "x") is available or is already operating, e.g., as a part of a high level action (HLA) which is under implementation;
  - $0 \rightarrow$The upper bound "∞" (or any large value representing the infinity) means that the system is known to be failed beyond repair.

"*Alternative*" in the Severa terminology represents one specific set (or a "vector") of values of TD terms. For illustration, Figure 5 compares the TD terms for systems (which are then translated to the TD terms for the success paths) for two different alternatives.

For V&V purposes, it is useful to have in mind the format in which the results of the prognostic part of Severa are provided: for each considered "alternative", Severa provides the conditional probabilities of four mutually exclusive categories of an outcome: RC-E, RC-I, RC-L, RC-N. As the categories are considered mutually exclusive, the four conditional probabilities sum to 1.0.

The results are presented both numerically and graphically. However, just to mention it, there is an issue which makes graphical presentation difficult: Quantitative results (probabilities) appear in the range of 3 or even 4 orders of magnitude, as illustrated by Figure 6. There is a possibility to use logarithmic scale for presentation of the results. However, this can be confusing in a stressful situation and not very suitable for intuitive interpretation of the results.

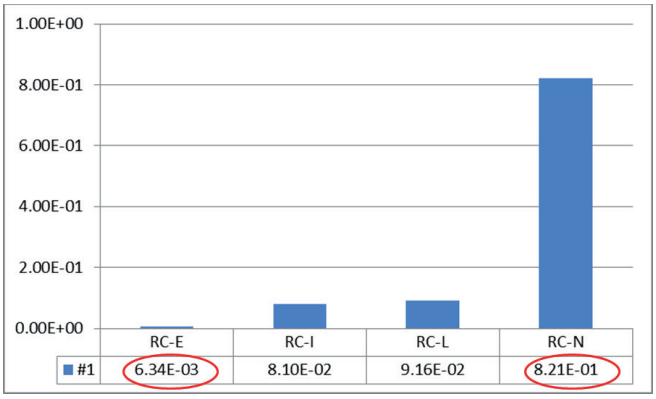

Fig. 6. Presentation of results – The range of probabilities of radioactive release categories

B. Approach to V&V

Two general aspects of any V&V can be described in a simplified way as:

1. *Verification:* check whether the product is in accordance with predefined specifications ("see whether you really got what you wanted");
2. *Validation:* check whether the product is suitable for the intended purpose / application ("see whether you really wanted what you got").

Usually, the second aspect is considerably more challenging than the first.

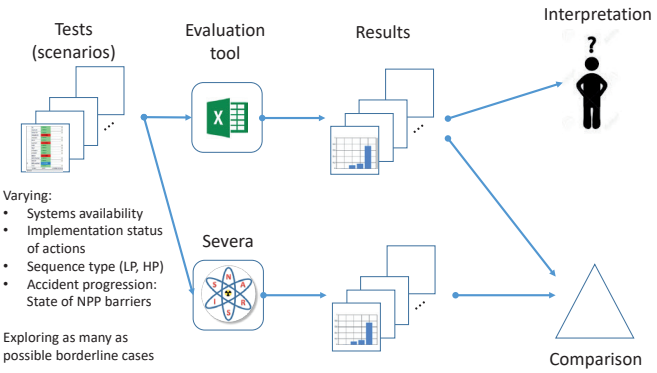

Fig. 7. Approach to verification and validation of Severa

The first step of the overall V&V of Severa was the deterministic verification and validation of possible recovery actions. It should be noted that a number of accident sequences were studied by MELCOR deterministic analyses [4] to evaluate phenomenological aspects of severe accidents, timing of important consequences without any recovery (operator) actions and success of performed recovery actions. According to [3] and [9], each SAG (SAG-1, SAG-2, SAG-3) is associated with a corresponding High-Level Action (HLA): HLA1, HLA2, HLA3. Each HLA contains several Success Paths (SPs), i.e., alternative and mutually exclusive ways of responding to the accident. Each SP uses one or more systems from the inventory of plan systems, such as pumps and power generators, which must be available and in a working condition in order to pursue the SP.

As already mentioned, two general types of severe accidents scenarios were studied in [4]: high pressure scenario and low pressure scenario. These two types generally differ with regard to the pressure behavior in the Reactor Coolant System (RCS) following the assumed initiating event (IE). For each of them, a number of deterministic analyses by MELCOR were performed.

Luka Štrubelj, Klemen Debelak, Marko Bohanec, Adem Kikaj, Ivan Vrbanić, Ivica Bašić, Use of Supporting Software Tool for Decision-Making During Low-Probability Severe Accident Management at Nuclear Power Plants, Journal of Energy, vol. 71 Number 4 (2022), 3–11
https://doi.org/10.37798/2022714423

The second part of the overall V&V process for Severa was established along the following lines (Figure 7):

- →Verification part for Severa tool. It was rather straightforward and consisted of the following activities:
  - o→Define test cases involving different formulas embedded in the tool;
  - o→Pre-calculate results independently (externally to Severa), e.g., by a spreadsheet;
  - o→Perform runs by Severa and compare;
- →Validation part for Severa tool:
  - o→Define test cases for different conditions predictable by supporting analyses or knowledge / experience;
  - o→Define the expectations with regard to results. Those were related to likelihood profile of containment failure / release categories;
  - o→Calculate the results and interpret / evaluate them against the expectations;
  - o→Do also sanity-checks against other test results;

The procedure which was followed for a particular test can be summarized with the six steps:

1. Define the test case;
2. Describe the expectations concerning the results;
3. Pre-calculate results independently;
4. Evaluate results against expectations and against other relevant tests under V&V;
5. Obtain corresponding results by Severa and compare against step 3;
6. Do any adjustments or corrections, if needed.

It should be noted that both verification part as well as validation part have resulted with certain (mostly although not necessarily minor) corrections and adjustments of tests and Severa itself. It also should be noted that a considerable number (275) of test cases were done and passed successfully.

To illustrate the process, we present an example involving a group of rather simple test cases / subcases.

C. Example of a V&V

All cases presented below for illustration purposes represent checks involving a comparison of different alternatives. The considered situation is as follows. The time point at which tests are made is the time point at which the SAMGs are entered, i.e., the time point is set shortly after reaching CET = 650°C. Specifically, this occurs at time point = 126 min at the Station Blackout time series. No management action is under implementation. Tested is a set of alternatives with different TDx terms for specified functions. In all cases the following applies:

- Large TDx (TD goes to infinity) is simulated with TDx = 60000 min;
- TDxy = TDx + TDy when restoring combinations of systems;
- For each HLA / Function: No function is under implementation.

Case 1.0. Zero Alternative, A0: All TDx Large

- Zero alternative is defined as: no function available and no actions will be taken (no recovery). Therefore: all TDx terms are large.
- Expectation: Release: RC-E if SG creep rupture, or RC-I if no SG creep rupture. If no SG creep rupture, containment is expected to fail in intermediate time window due to mass and energy release (MER) challenge.
- Results: As below. Considered OK. Reproduced by Severa OK.
-

RC-E	RC-I	RC-L	RC-N	
1.06E-02	9.89E-01	0.00E+00		0.00E+00

Case 1.1. Comparing Different Subcases with Availability (at TD = 0) of HLA1, HLA2 and / or HLA3. (No Containment Heat Removal)

For this case, the initial / underlying conditions and assumptions are the same as under the Case 1.0 above. Various subcases which were then quantified reflect the assumption that particular function / combination of functions became available with TD = 0 (i.e., became available "now", at the time a decision is to be made). For example, in the Subcase 1.1.1 below it is assumed that the function "inject to SG" (HLA1) becomes available, while all other conditions are as under the Case 1.0 above. Presented below, for illustration, are two subcases: the mentioned Subcase 1.1.1, and the Subcase 1.1.7 under which it was assumed that a combination of critical functions becomes available with TD = 0. The purpose of all subcases under this Case 1.1 was to see whether the quantified results fulfill the expectation when compared against the initial results from the Case 1.0.

Subcase 1.1.1: HLA1 (Inject to SGs)

- Expectation: This HLA can address SG creep rupture and reduce the likelihood of early release (RC-E). However, it cannot address containment challenge in later time frames. Primary inventory will be lost through the Reactor Coolant Pump (RCP) seals and Pressurizer PORVs. Thus, reactor vessel failure (VF) and containment challenge cannot be avoided and they are expected at intermediate time frame. Therefore: RC-E probability decreases on account of RC-I. RC-L = RC-N = 0.
  - o→The best option, according to the assumptions, is AFW. (This is because it is a design-basis safety system, with most strict design, installation and maintenance requirements.) Thus, this option is expected to give the smallest RC-E probability. For other options RC-E probability increases.
- Results: As shown in Table I. Considered OK. (Note that the row #0 shows the results from the Case 1.0 above, for comparison.) Reproduced by Severa: OK. It is noted that graphical presentation is not very useful for comparing cases like these (Figure 8), because the results may cover the range of several orders of magnitude.

Luka Štrubelj, Klemen Debelak, Marko Bohanec, Adem Kikaj, Ivan Vrbanić, Ivica Bašić, Use of Supporting Software Tool for Decision-Making During Low-Probability Severe Accident Management at Nuclear Power Plants, Journal of Energy, vol. 71 Number 4 (2022), 3–11
https://doi.org/10.37798/2022714423

TABLE I.

V&V EXAMPLE (SUBCASE I.I.I)

#	TDx = 0	RC-E	RC-I	RC-L	RC-N
0	Zero (All TD>>)	1.06E-02	9.89E-01	0.00E+00	0.00E+00
A	(AFW)	1.50E-03	9.99E-01	0.00E+00	0.00E+00
B	(SGPORV) (DECSG)	1.90E-03	9.98E-01	0.00E+00	0.00E+00
C	(DECSGPORV) (DECSG)	2.40E-03	9.98E-01	0.00E+00	0.00E+00
D	(SGPORV) (FLEXSG)	2.70E-03	9.97E-01	0.00E+00	0.00E+00
E	(DECSGPORV) (FLEXSG)	3.30E-03	9.97E-01	0.00E+00	0.00E+00

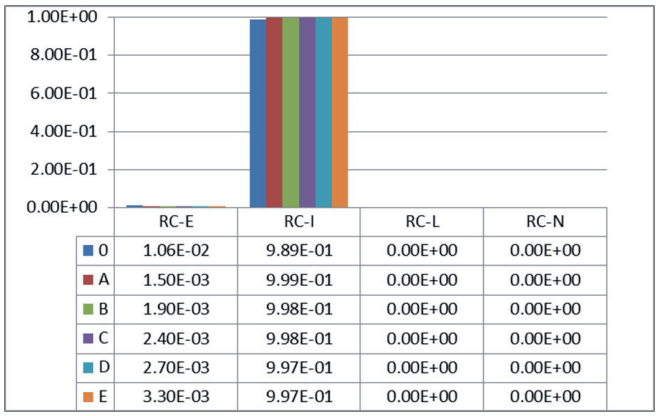

Fig. 8. V&V example (Subcase I.I.I) - Graphical presentation

Subcase 1.1.7: Combined HLA1 /HLA2 with HLA3I / HLA3R (SG Flooded / RCS Depressurization and RCS Injection / Recirculation)

- →Expectation: With RCS depressurized and injection / recirculation available, there is a possibility to achieve in-vessel recovery (IVR). However, there is no containment heat removal. Containment will fail under RC-I only if IVR is unsuccessful and challenge to containment develops. Otherwise: long term concern.
  - o→Therefore, expectation for all options is: RCE-E low (SG flooded). Containment failure at RC-N (most likely) or RC-I.
  - →Note: RC-L is not expected: if IVR fails then RC-I expected. If IVR successful then long term concern applies.
  - →Results: As shown in Table II. Considered OK. In accordance with expectations.
  - o→Note, also: Split between RC-I and RC-N is in accordance with adequacy of available HLA3 function: Probability of RC-I(LPSI) is smaller than probability of RC-I(DEC), which in turn is smaller than probability of RC-I(FLEX) (Figure 9).

D. IMPLEMENTATION OF V&V

In order to run V&V tests, a special software module was added to Severa. After loading some time series (such as Station Blackout), the user can iteratively load test scripts, which are run by Severa, comparing the achieved radioactive release results with the ones obtained by the alternative evaluation tool and prescribed in scripts.

A test script is a JSON (JavaScript Object Notation) data file that contains a description of multiple hypothetical alternatives together with their expected radioactive releases. Each test/alternative is described by a number of data items that set up the hypothetical environment (time series data, the current time point) and the states of plant systems (in terms of TD and completed actions).

TABLE II.

V&V EXAMPLE (SUBCASE I.I.7)

#	TDx = 0	RC-E	RC-I	RC-L	RC-N
0	Zero (All TD>>)	1.06E-02	9.89E-01	0.00E+00	0.00E+00
	HLA1 and HLA3I / HLA3R				
A	(AFW) (LPS) (SMPLPSI)	1.27E-03	3.00E-02	0.00E+00	9.69E-01
B	(SGPORV) (DECSG) (LPSI) (SMPLPSI)	1.67E-03	3.00E-02	0.00E+00	9.68E-01
C	(DECSGPORV) (FLEXSG) (LPSI) (SMPLPSI)	3.08E-03	6.83E-02	0.00E+00	9.29E-01
D	(AFW) (DECSI) (SMPDECSI)	1.28E-03	1.27E-01	0.00E+00	8.72E-01
E	(DECSGPORV) (FLEXSG) (FLEXRCS) (SMPFLEX)	3.11E-03	3.47E-01	0.00E+00	6.50E-01

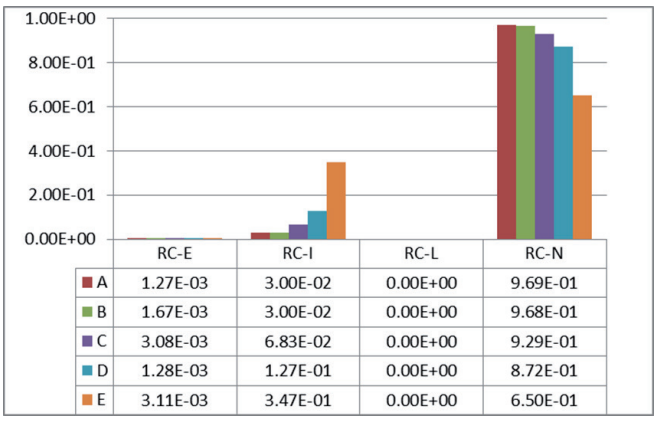

Fig. 9. V&V example (Subcase I.I.7) - Graphical presentation

V. CONCLUSION

Severa is a proof-of-concept tool which was developed with an idea to investigate the feasibility of using a computer decision-support tool in severe accident management, primarily for the training of NPPs Technical Support Center (TSC) staff. The demonstration version of Severa is capable of evaluating potential successes of available severe accident management guideline (SAG) action courses, based on the assumed time windows for successful recovery actions and predetermined probability profiles of expected major radioactive release categories for different plant status / configurations. The appropriate timely executed operator actions should reduce the early containment failure or/and minimize other types of radiological releases. The TSC staff decisions based on additional information and training with Severa tool can lead to better understanding and management of severe accidents in nuclear power plants. Although the prototype version is largely simplified with regard to the real situations, the extensive verification and validation exercises showed that it can provide reasonable predictions of probability profiles of major release categories for the scenarios considered.

With regard to the limitations in probabilistic risk quantifications, it is important to recognize that the objective of the tool itself is not to calculate the "realistic" or best estimate probabilities of releases associated with particular alternative being evaluated. Rather, the objective is to be able to learn which alternatives are relatively better than the others. In any case, this definitely repre-

Luka Štrubelj, Klemen Debelak, Marko Bohanec, Adem Kikaj, Ivan Vrbanić, Ivica Bašić, Use of Supporting Software Tool for Decision-Making During Low-Probability Severe Accident Management at Nuclear Power Plants, Journal of Energy, vol. 71 Number 4 (2022), 3–11
https://doi.org/10.37798/2022714423

sents an opportunity for future improvements, particularly the time dependency of the release category probability matrix, which would enable using the tool also in the later phases of accident management.

VI. Acknowledgments

The work in the project NARSIS is supported by European Commission, Directorate general research & innovation, by grant agreement 755439. Marko Bohanec also acknowledges the financial support from the Slovenian Research Agency, research core funding No. P2-0103.

References

[1] L. Štrubelj, E. Foerster, G. Rasitello, J. Daniell, B. Bazargan-Sabet, P. Gehl, P. J. Vardon, V. K. Duvvuru Mohan, "The Goal of the New Approach to Reactor Safety Improvements (NARSIS) Project", Proceedings of the 12th International Conference of the Croatian Nuclear Society, Zadar, Croatia, 3-6 June 2018

[2] K. Debelak, L. Štrubelj, I. Bašić, "Report on characterized EOP/EDMG/SAMG – Deliverable 5.2", NARSIS project, 2018

[3] I. Vrbanić, I. Bašić, L. Štrubelj, K. Debelak, M. Bohanec, "Definition of Hazard-Induced Damage States and Development of State-Specific APETs for Demonstration Purposes – Deliverable 5.3", NARSIS project, 2019

[4] P. Darnowski, P. Mazgaj, I. Bašić, I. Vrbanić, M. Skrzypek, J. Malesa, A. Silde, J. H., L. Štrubelj, Severe Accident Simulations Dedicated to the SAMG Decision-Making Tool Demonstration, NENE-2020, 2020

[5] M. Bohanec, A. Kikaj, I. Vrbanić, I. Bašić, K. Debelak, L. Štrubelj, "Supporting Severe Accident Management in Nuclear Power Plants", ICDSST 2020, Zaragoza, Spain, 27.5-29.5.2020

[6] M. Bohanec, I. Vrbanić, I. Bašić, K. Debelak, L. Štrubelj : A decision-support approach to severe accident management in nuclear power plants. Journal of Decision Systems, 13 p., 2020, doi: 10.1080/12460125.2020.1854426.

[7] N. Trdin, M. Bohanec: Extending the multi-criteria decision making method DEX with numeric attributes, value distributions and relational models. Central European Journal of Operations Research, 26(1), 1–41, 2018. doi:10.1007/s10100-017-0468-9

[8] Bohanec, M.: DEX (Decision EXpert): A qualitative hierarchical multi-criteria method. Multiple Criteria Decision Making (ed. Kulkarni, A.J.), Studies in Systems, Decision and Control 407, Singapore: Springer, doi: 10.1007/978-981-16-7414-3_3, 39-78, 2022

[9] M. Bohanec, I. Vrbanić, I. Bašić, D5.4a - Supporting SAMG DM tool for demonstration purposes, NARSIS Deliverable, 2021

Journal of Energy
VOLUME 71 Number 4 | 2022
journal homepage: http://journalofenergy.com/

On Minimal Cut Sets Representation with Binary Decision Diagrams

Reni Banov, Zdenko Šimić

***Summary* — Since their introduction in form of a canonical representation of logical functions, the Binary Decision Diagrams (BDDs) gained a wide acceptance in numerous industrial applications. This paper summarizes the properties of BDD representation of Minimal Cut Sets (MCS) of Fault Tree (FT) models most typically encountered in nuclear energetics. Cut sets from MCS are defined as paths from the top BDD node to terminal nodes in the BDD, on which a quantitative and qualitative FT analysis (FTA) is performed. The core of the FTA on the BDDs is performed with help of two fundamental algorithms, one for conditional probability evaluation and another for the selection of cut sets. The accuracy of conditional probability evaluation represents an essential feature for an unbiased quantitative analysis, such as the top event probability or the determination of event importance measures. The cut set selection algorithm is shown in a generic version introducing logical predicates for its selection criteria. As it is known, the efficiency of depicted algorithms depends only on the number of BDD nodes used for the FT representation. In order to appraise the compactness of the BDD representation of FT models, their characteristics have herein been evaluated on several real-life models from the Nuclear Power Plant Krško. The extraordinariness of the compactness of the BDD representation reflects in its ability to implement advanced dynamic analysis (i.e. what-if) of FT models. The efficiency of such an approach is recognized by commercial vendors upgrading their FT Tools to new versions by implementing BDD based algorithms.**

***Keywords* — Probabilistic Safety Assessment (PSA), Fault Tree Analysis (FTA), Binary Decision Diagrams (BDD), Minimal Cut Sets (MCS)**

I. Introduction

Introduced in the early 60's as a tool for analysing failure conditions of military systems [1], the Fault Tree Analysis (FTA) has become one of the most popular methods to deductively analyse undesired behaviour of complex engineering systems from various industries. The static Fault Tree (FT) is a directed acyclic graph (DAG) with a single top node representing a failure event under analysis. Terminal nodes at the bottom of the FT are basic events representing a component failure occurrence and are considered relevant for the analysis. The intermediate nodes are conditions under which the basic events propagate their occurrence to the top node. An example of a simple FT is given in Figure 1. In a general view to FTA, we differentiate two types of static analysis: the qualitative and the quantitative [2]. Under the qualitative analysis the FT is typically evaluated to find minimal cut sets, minimal path sets, and common cause failures. Quantitative analyses are performed numerically with the goal of computing various reliability measures, like system availability, mean time between failures, component importance measures, and others.

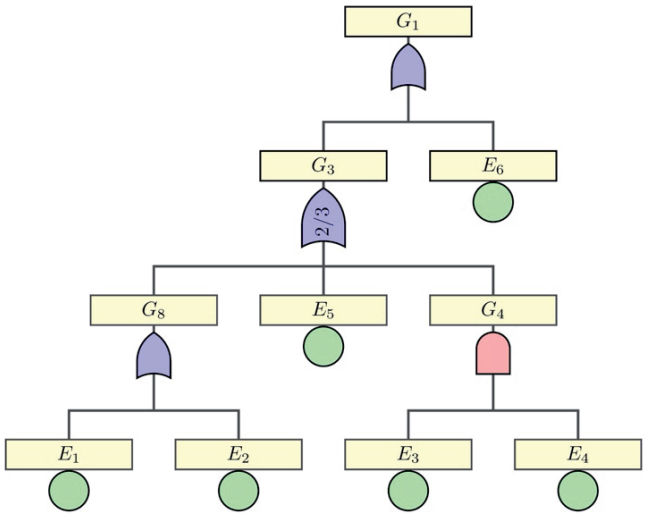

Fig. 1. Fault Tree example

It should be brought to attention that the FT structure represents a large Boolean function which depends on the occurrence of basic events, thereby allowing their minimization to find representation in form of minimal cut sets (MCSs). The conventional approach to FTA relies on a process of determination of minimal cuts sets from the FT structure by applying a simplification rule according to the Boolean laws. The two most common conventional approaches are based on top-down or bottom-up rewritings of logical formulas defined by intermediate FT nodes. Both approaches are computationally intensive and are resource demanding, and may, thereby, be applied only to determine the most significant minimal cuts based on probability values or their size. Lately, the new techniques are constructed on Binary Decision Diagrams (BDDs) [3, 4] and Monte Carlo [5] simulation methods. The BDD method of minimization of Boolean functions seems to be more powerful than Monte Carlo methods, though it depends on the knowledge of a good basic event order to achieve supremacy [6]. The advantage of

(Corresponding author: Reni Banov)
Reni Banov is with the University of Applied Sciences (TVZ) Zagreb, Croatia (e-mail: reni.banov@tvz.hr)
Zdenko Šimić is with the Energy Institute Hrvoje Požar (EIHP) Zagreb, Croatia (e-mail: zsimic@eihp.hr)

Monte Carlo simulation methods is that they can be easily applied to the dynamic fault tree (DFT) analysis.

However, finding the minimal form of any Boolean function is a NP-complete problem, even for the simplest case of monotonic Boolean functions. The time and space complexity of a problem requires a novel data structure to represent Boolean functions. Normally, Boolean functions are represented by truth tables or logical expressions, but the BDD structure, i.e., a variant of DAG with two terminal vertices, are far more efficient for implementation. The BDDs for Boolean functions are derived from the Shannon identity

$$f(\boldsymbol{x}) = \left(x_i \wedge f(\boldsymbol{x}; 1_i)\right) \vee \left(\neg x_i \wedge f(\boldsymbol{x}; 0_i)\right) \quad (1)$$

applied recursively to each function in expansion. Each Shannon step generates a part of a full binary tree with vertices structured, as shown in Figure 2, down to the bottom of the tree with two terminal vertices representing Boolean values {**0**,**1**}.

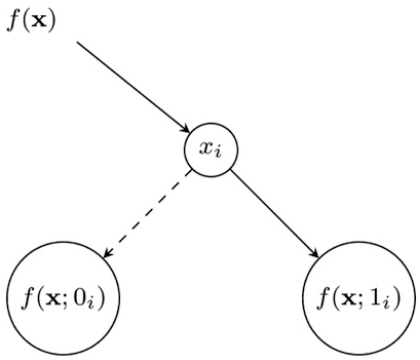

Fig. 2. Shannon identity step as binary tree

The Shannon identity with BDDs is commonly expressed by means of the If-Then-Else (*ite*) construction, for instance, the tree structure of the function from Figure 2 is written as

$$ite(x_i, f(\boldsymbol{x}; 1_i), f(\boldsymbol{x}; 0_i)) \quad (2)$$

If an order of variables is the same (preserved) on each path from any vertices down to terminal vertices, the BDD is denoted as *ordered* BDD [7]. During the Shannon expansion the vertices for each unique Boolean function are generated only once, thereby making an ordered BDD reduced and ensuring the uniqueness of representation, i.e., the canonical representation of the Boolean function. The BDD structure allows an efficient implementation of usual logical operations, which makes it a suitable tool for manipulating Boolean functions.

II. BDD Method for MCS Set

From the very beginning of the application of fault tree analysis in nuclear energetics it has clearly come to mind, that a more accurate insight into the reliability of the observed system relies on the understanding of the complete or, at least, the most significant parts of failure sets (minimal cut sets MCSs). However, the determination of MCSs turns out complex even with very simple systems modelled by a coherent fault tree, dealing with at least two hard problems. The first, being the time complexity of algorithms employed for the determination of the complete or partial set of MCSs, while the second relates to a space complexity of the same sets recording. More recently binary decision diagrams (BDDs) have been developed, enabling an indirect recording of fault trees by applying indicator variables for the component failure state within the system.

The basic idea behind the BDD method is to define an indicator variable which acquires the logical value zero (false) if the basic event does not occur, and inversely, the logical value one (true) if the basic event occurred. The probability of the basic event occurrence is thereby associated with the probability of true occurrence of the indicator variable. In this way the Bernoulli random variable is assigned to the basic event. Once the logical function represented by the FT is converted to a BDD representation, the BDD based method [3] can be used to find its minimal disjunctive form which represents a MCS set of the coherent FT. Figure 3 shows the BDD representation of the complete MCS set of the FT example from Figure 1. The dotted arrow line marks that the MCS does not include the event originating from the line, while the full arrow line stands for the event included in MCS. The full MCS set is defined by all paths from the top node ending at the node with value one (true). It is worthwhile mentioning that non-coherent FTs can be treated similarly with Zero Decision Diagrams (ZDDs) which are a variant of BDD supporting combinatorial sets [8].

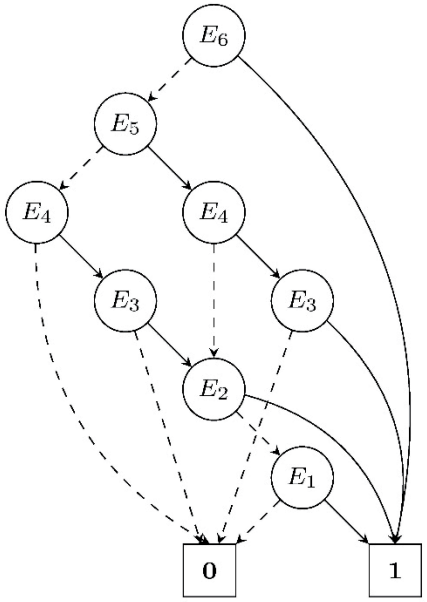

Fig. 3. MCS as BDD tree

Once the BDD of the MCS set is created, an analysis can be performed on indicator variables with algorithms specifically written for the BDD structure. The qualitative analysis relies on the selection of MCS sets according to specific criteria. This kind of analysis is easily performed based on the algorithm which can select a subset of MCSs from BDD with predicates applied to the indicator variables. The underneath algorithm (Figure 4) implements a subset selection from the full MCS set represented by the BDD structure defined on indirect variables.

The essence of the algorithm is to select from a full MCS set only cut sets for which the predicate results in true value on indirect variables. With a new minimal cut set the decision is rather simple, namely, as soon as the terminal node with value one is reached, the predicate on truth values of indirect variables traversed through the path can be applied. This part of the algorithm is entailed in lines 9-14. Not having reached the terminal node means that we still dwell on a node determined by a single indirect variable (a single basic event). Subsequently, we can pursue the traversal of

the BDD graph via the branch containing that variable (full arrow line), assuming that the predicate responded in value one (true) for the part of the cut set found. Contrary to that, on a zero (false) responded value the traversal is carried on with the branch not containing that variable (dotted arrow line). This part of the algorithm from Figure 4 is displayed in lines 16-20. The lines 6-8 from the algorithm represent paths leading to the zero terminal node, i.e., to the node indicating that the minimal cut set has not been found through the path. It is important to mention that the predicate for the cut set selection must return a logical value even if only a part of the minimal cut set stands. For example, predicates conforming to that criteria are typical predicates used for the analysis, such as a maximal number of basic events in a cut set or a minimal cut set probability value.

The cut set probability evaluation is performed with the assumption that basic events are independent, in other words, the probability value of a cut set equals to the product of probabilities of basic events contained in the cut set. Basically, by introducing line 17 in the algorithm a significant reduction of the traversal has been performed resulting in a reduction of the execution time for the minimal cut set selection. What is more, by introducing the concept of predicates for the cut set selection we have achieved a flexibility for the creation of complex selection criteria since logical expressions defined by predicates can be combined with common logical operators. For example, it is rather easy to specify criteria containing cut sets which bear a specific number of basic events and meet either conditions of a minimal probability value or conditions containing a specific basic event. In this way we have achieved a significant flexibility to perform a highly specific qualitative and quantitative FT analysis.

Input: $MCS(v_m, mcs, F, cs)$
Output: $mcs \leftarrow MCS(v_m, F)$

```
1  v_m ∈ V_mcs                                          // MCS set BDD top node
2  mcs = {cs_i}                                         // MCS subset selected with predicate F
3  F: {E_i} → 𝔹                                         // Selection criteria as predicate
4  cs = {E_i}                                           // Current cut set
5  begin
6      if value(v_m) = 0 then
           /* Terminal node 0                                                    */
8          return
9      else if value(v_m) = 1 then
           /* Terminal node 1                                                    */
10         if F(cs) = 1 then
               /* Predicate is fullfiled with current cut set cs                 */
12             mcs = mcs ∪ cs
14         return                                       // Terminal node 1 ends current cut set
15     else
           /* E_index(v_m) basic event indirectly specified with index(v_m)      */
16         if F(cs ∪ {E_index(v_m)}) = 1 then
18             return MCS(high(v_m), mcs, F, cs ∪ {E_index(v_m)})
20         return MCS(low(v_m), mcs, F, cs)
```

Fig. 4. MCS subset selection

The second basic algorithm (Figure 5) represents the calculation procedure of the conditional probability from the paths in the BDD graph. Analogously to the previous algorithm the BDD structure is traversed in a depth first manner and conditional probabilities are calculated from indicator variables encountered on the traversal path. Whenever we reach terminal nodes we need to return the probability value confirmed by the truth value of terminal nodes, thus, for terminal node one the value 1.0 is returned, while for terminal node zero the value 0.0 is returned. This part of the algorithm is set forth in lines 5-10. Once an intermediate node is reached, by checking the truth value of the indicator variable from the parameter set (σ), we may decide on the continuance of the BDD traversal. Thus in lines 14-16 the traversal is continued in case of a zero (false) value indicator variable, i.e., in this case we are calculating the conditional probability provided that the basic event associated with the indicator variable did not occur. Similarly to that, in lines 17-19 the conditional probability is calculated assuming that the particular basic event has occurred. In all other cases we continue with a recursive calculation of the conditional probability by traversing the BDD structure on left and right branch nodes (line 22). It is essential to mention that the significant algorithm optimisation may be achieved by saving the intermediate result of the conditional probability calculation for that node. In this way a multiple calculation of conditional probabilities for the same nodes encountered during the traversal is avoided, which at the end, results in time efficient computation.

Input: $\Pr(v_f, \sigma)$
Output: $p \leftarrow P(\sigma(f) = 1)$
Data: $\sigma(f)$ set of indicator variables with known state

```
1  begin
2      if value(v_f) = 0 then
4          return 0                                     // Terminal node 0
5      else if value(v_f) = 1 then
7          return 1                                     // Terminal node 1
8      else
           /* probability of basic event E_index(v_f)                            */
10         p_i ← P(E_index(v_f) = 1)
11         if σ(index(v_f)) = 0 then
13             return (1 − p_i) · Pr(low(v_f), σ)       // Basic event E_index(v_f) = 0
14         else if σ(index(v_f)) = 1 then
16             return p_i · Pr(high(v_f), σ)            // Basic event E_index(v_f) = 1
17         else
               /* Unknown state of the basic event E_index(v_f)                  */
19             return
                   Pr(low(v_f), σ) + p_i · [Pr(high(v_f), σ) − Pr(low(v_f), σ)]
```

Fig.5. Indirect evaluation of conditional probability from BDD

Now, a qualitative and quantitative analysis on a fault tree model may be carried out with BDDs by applying known algorithms for the determination of a minimal disjunctive normal form of the logical function presented by the coherent fault tree, which represents the logical recording of a set of minimal cuts.

III. Results and Discussion

The previous algorithms are implemented in the C/C++ programming language and their correctness and accuracy has been tested on FT models from the nuclear power plant Krško. For the implementation of the BDD algorithm it was necessary to find a good basic event order by which the BDD representation of the FT may be traced. The following table brings characteristics of FT models (column *B.E.* stands for the number of basic events, column *Gates* is the number of intermediate events) utilized in the testing as well as properties of the BDD representation of their complete MCS set.

Table I
Results on NEK FT test models

FT	B.E.	Gates	BDD	MCS	Ratio MCS/BDD
acp	409	674	4.583	228.242.636	49.802
chrgr	438	695	68.904	14.840.731.139.897	215.382.722
dcp	447	706	77.595	152.148.878.846.392	1.960.807.769
efw	692	957	265.401	1.769.960.840.506.752	6.669.005.921
hpsi	674	940	22.902	371.554.422.700	16.223.667
lpsi	525	760	26.754	479.582.239.771	17.925.627
sw	444	720	140.486	58.952.275.075.664	419.630.960
cored1	1319	1279	1.951.673	69.273.024.997.243.046	35.494.176.020
cored2	1377	1633	16.524.072	2.436.058.751.633.933.343	147.424.844.895

Reni Banov, Zdenko Šimić, On Minimal Cut Sets Representation with Binary Decision Diagrams, Journal of Energy, vol. 71 Number 4 (2022), 12–15
https://doi.org/10.37798/2022714420

The number of cut sets in MCS set (column *MCS*) for the tested FT models ranges between 10^8 and 10^{18}, while the BDD size (column *BDD*) for the most complex model (cored2) comes to 16.5 million nodes. Since the nodes are represented with a structure of 32 bytes sized we can conclude that the full MCS set for the most complex model shall need approx. 500MB RAM memory. It is hard to conceive how much memory it would take for conventional FTA programmes to represent a complete MCS set of the cored2 model.

Apart from the compact representation, the BDD structure allows an efficient execution of the mentioned algorithms; e.g., the selection of the MCS subset according to predicate criteria for a cut set length equalling to 5 basic events lasts for approx. 2 seconds on a desktop PC with 8GB RAM and an Intel i5 processor. The execution time of the algorithm is predominantly influenced by the selection of the traversal branch which does not meet the predicated condition, i.e., on the branch with a basic event for which the predicate returns a false value in the early traversal phase (see line 16 of algorithm in Figure 4).

Also, the top event conditional probability calculation by means of the algorithm from Figure 5 takes on an average less than one second even for the probability of a top event without any condition on indicator variables. This is the most complex case, since BDD traversals are performed through each node. However, once the result for every node is saved (a single double precision number) we can reuse the calculated result which significantly speeds up the calculations, as by this the complexity of the algorithm becomes proportional to the number of nodes in the BDD. Effectively, for the most complex model we achieved the worst case complexity of order double precision operations. The *n* in the complexity order represents the number of nodes from the BDD. The above written indicates an outstanding compact BDD representation (column *Ratio MCS/BDD*) of the MCS set and a remarkably efficient implementation of the analysis algorithm. The respective column indicates the average quantity of paths going through a BDD node.

Recently [9], besides the BDD representation compactness the results of the quantitative analysis performed on BDDs were thoroughly compared to the results obtained with conventional FTA tools. The authors compared the results obtained by means of these two techniques (conventional and BDD) on the Liebstatdt NPP model (KKL) and found some interesting outcomes. For example, they established that a "*substantial reduction in CDF/FDF was achieved for KKL PSA model*" signifying that the application of the BDD approach may have potential on the reduction of risk metrics in other models, too. It is worthwhile mentioning that the BDD quantitative analysis approach results in exact values, thereby not having any biases commonly occurring with conventional approaches.

IV. Conclusion

The preparation of the basic event ordering for the application of BDD methods makes the most important task of the analysis based on the BDD structure. The ordering procedure alone is the principal time consuming task; luckily it is performed only once and does not have to be repeated for other calculations. Along with the ordering, the MCS set is also computed once and needs not to be repeated unless the structure of the FT model has been changed. The exceptional compactness of minimal cut set recordings gained by the BDDs technique ensures the recording of a complete set of MCSs. The complete MCS set is defined by a logical function on indicator variables defined from the FT model. Once the complete MCS set has been found, the analysis is repeatedly performed by changing the conditions. For example, changing the probability of a basic event occurrence or defining different selection predicates enables a repeated analysis without MCS set re-determination.

The most distinguished advantage of the BDD based FTA is its compact representation and the fact that the qualitative and quantitative analysis can be performed on complete MCS sets. Actually, the numerical precision of the calculations does not depend on the number of cut sets in the MCS set entirely unlike conventional FTA approaches that must re-compute a part of the MCS set and perform analysis thereon.

Another important feature of BDD based algorithms is that their complexity is proportional to the number of BDD nodes and by this, they do not depend on the number of cut sets in the complete MCS set. Thus, not only do BDDs show (under the condition of an appropriate variable order) an acceptable time complexity for the implementation of algorithms for determining and analysing MCSs but also enable a compact recording of complete or partial sets of MCSs singled out in that way. Along with this, the compact BDD representation allows the development of new and improved analysis techniques since a complete MCS set is available for the implementation of such algorithms. This circumstance opens new prospects for further research and development of BDD analysis methods, especially in the field of nuclear energetics which utilizes the most complex FT models.

References

[1] C.A. Ericson, "Fault Tree Analysis – a history", *In Proceedings of the 17th International System Safety Conference*, Orlando, Florida, USA, 16-21 August 1999, pp. 1 – 9

[2] E.J.J. Ruijters, M.I.A. Stoelinga, "Fault Tree Analysis: A survey of the state-of-the-art in modeling, analysis and tools", CTIT TR-CTIT-14-14, Centre for Telematics and Information Technology, University of Twente, NL., 2014.

[3] A.B. Rauzy, "New algorithms for fault tree analysis", *Reliability Engineering & System Safety*, Vol. 40, No. 3, pp. 203–211, 1993.

[4] R. Remenyte-Prescott, J.D. Andrews, "An enhanced component connection method for conversion of fault trees to binary decision diagrams", *Reliability Engineering & System Safety*, Vol. 93, No. 10, pp. 1543–1550, 2008.

[5] K. Durga Rao, V. Gopika, V.V.S. Sanyasi Rao, H.S. Kushwaha, A.K. Verma, A. Srividya, "Dynamic fault tree analysis using Monte Carlo simulation in probabilistic safety assessment", *Reliability Engineering & System Safety*, Vol. 94, No. 4, pp. 872–883, 2009.

[6] R. Banov, Z. Šimić, D. Grgić, "A new heuristics for the event ordering in binary decision diagram applied in fault tree analysis", *Proceedings of the Institution of Mechanical Engineers, Part O: Journal of Risk and Reliability*, Vol. 234, No. 2, pp. 397–406, 2020.

[7] R.E. Bryant, "Graph-Based Algorithms for Boolean Function Manipulation", *IEEE Transaction on Computers*, Vol. 38, No. 8, pp. 677–691, 1986

[8] O. Coudert, J.C. Madre, "Metaprime: An interactive fault-tree analyzer", *IEEE Transaction on Reliability*, Vol. 43, No. 1, pp. 121–127, 1994

[9] P. Zvoncek, O.Nusbaumer, "Comparison of MCUB and MCS BDD Fault Tree Solution Algorithms using Liebstadt Nuclear Power Plant Model", *PSAM 14*, Los Angeles, CA, USA, 16-21 September 2018

Journal of Energy

VOLUME 71 Number 4 | 2022

journal homepage: http://journalofenergy.com/

The progression of Guarantees of Origin trading in Croatia amidst the European framework

Marko Kelava, Martina Vajdić, Boris Dokmanović

***Summary* — This article explores the progress and development of Guarantees of Origin trading in Croatia, specifically focusing on the regulatory framework implemented by the Republic of Croatia. The responsibility for issuing Guarantees of Origin for electricity and managing the Registry of Guarantees of Origin lies with the CROATIAN ENERGY MARKET OPERATOR Ltd. (HROTE). The Croatian Registry of Guarantees of Origin was established in 2014, and full implementation commenced in February 2015 with the registration of the first users.In alignment with the Law on Renewable Energy Sources and Highly Effective Cogeneration, HROTE, as the leader of the ECO Balance Group for incentivized electricity production, began selling a portion of the energy produced on the trading platforms of CROATIAN POWER EXCHANGE Ltd. (CROPEX) since the beginning of 2019. This shift towards market-based electricity sales created an opportunity to establish a system for trading Guarantees of Origin, specifically for electricity produced by eligible incentivized producers and sold on CROPEX markets by HROTE. The issuance of Guarantees of Origin for relevant power plants occurs within the Croatian Guarantees of Origin Registry, where they are sold to market participants based on market principles through Guarantees of Origin Auctions. CROPEX organizes these auctions using a specially developed IT auction trading platform. Once an auction is successfully completed, the raised funds are transferred to the incentivized system fund, and the sold Guarantees of Origin are transferred from HROTE's account in the Guarantees of Origin Registry to the user accounts of the auction participants. Overall, Guarantees of Origin empower end customers to determine the source of their supplied electricity, enabling them to make informed choices. This energy certification process verifies that consumers have purchased energy from renewable sources. Guarantees of Origin also serve as effective tools for promoting the use of renewable energy sources and attracting investments in renewable energy generation. Consequently, they contribute to achieving targets related to renewable energy utilization. The article also delves into the background and development of Guarantees of Origin trading in Croatia, positioning the country as a leader in this domain within the European context. It includes a comparative analysis of the Guarantees of Origin market in the United Kingdom as a reference point, with consideration given to the impact of Brexit on Guarantees of Origin markets. Additionally, the article explores the segregation of Guarantees of Origin auctions based on specific technologies and their characteristics. For instance, Guarantees of Origin from biomass power plants are sold through two different auctions based on the plant's installed capacity, while Guarantees of Origin from wind power plants are also sold through two auctions, but contingent on the commissioning start date. These distinctions lead to varying prices depending on the technology's age or installed capacity.**

***Keywords* — Guarantees of Origin, Energy certification, trading, auction, renewable energy sources, high-efficiency cogeneration, CROATIAN POWER EXCHANGE Ltd. (CROPEX), CROATIAN ENERGY MARKET OPERATOR Ltd. (HROTE)**

1. INTRODUCTION

Conducting auctions of Guarantees of Origin in Croatia refers to electricity produced in the production facilities of eligible electricity producers who have a valid contract for the purchase of electricity concluded in accordance with the Tariff System for production of electricity from renewable energy sources and cogeneration.[1]

CROATIAN ENERGY MARKET OPERATOR Ltd. (HROTE) determines the number of Guarantees of Origin (GO) it sells at auctions of Guarantees of Origin in accordance with the definitions and provisions of the Decree on the Establishment of the System of Guarantees of Origin of Electricity (Official Gazette 28/23).[1]

Guarantees of Origin HROTE sells at auctions conducted by CROATIAN POWER EXCHANGE Ltd. (CROPEX). CROPEX is the central contracting party that enables the sale of Guarantees of Origin by matching the bids of the auction participants with the offer of HROTE for the sale of the number of Guarantees of Origin at auction through the auction system.

To participate in the auction of Guarantees of Origin at CROPEX, each participant in the auction with an agreement on participation in the auction of Guarantees of Origin must have an account in the Croatian Register of Guarantees of Origin maintained by HROTE or in one of the registers of Guarantees of Origin affiliated to the AIB (Association of Issuing Bodies) system hub. AIB is a Brussels-based organization that regulates the European energy certification system, the so-called EECS (European Energy Certificate System) [2], to which HROTE joined as a full member on 23 May 2014.[1]

(Corresponding author: Marko Kelava)

Marko Kelava, Martina Vajdić are with the Croatian Power Exchange Ltd. (CROPEX) Zagreb, Croatia, (e-mails: marko.kelava@cropex.hr, martina.vajdic@cropex.hr)

Boris Dokmanović is with Croatian Energy Market Operator Ltd. (HROTE), Zagreb, Croatia , (e-mail: boris.dokmanovic@hrote.hr)

Marko Kelava, Martina Vajdić, Boris Dokmanović, The progression of Guarantees of Origin trading in Croatia amidst the European framework, Journal of Energy, vol. 71 Number 4 (2022), 16–22
https://doi.org/10.37798/2022714457

II. Guarantees of Origin in the Wider European Context

Although the paper is dedicated to Guarantees of the Origin of electricity in the Croatian context, this short chapter provides an overview of the wider European context. This context is primarily related to the Clean Energy for All Europeans package, which promotes the three main objectives of European policy:

- putting energy efficiency first,
- achieving global leadership in renewable energy sources,
- providing a fair deal for consumers.[2]

In the energy markets of the future, consumers will play an active and central role, including in the electricity market. Consumers across the EU will have a better basis for supply choices, access to reliable energy price comparison tools and the ability to produce and sell their own renewable electricity. Increased transparency and better regulation give citizens more opportunities to become more involved in the energy system.

Furthermore, the importance of energy policy issues is growing around the world, especially those related to clean energy and energy efficiency. Policy instruments that support the monitoring of energy sources and the disclosure of this information to consumers will play a key role in the transition to a sustainable future.[2]

Within the EU, unique GO issued in accordance with EU directives have the function of proving to the end customer the source of energy from which the energy they consume is produced. Guarantees of Origin can be transferred between account holders regardless of the energy to which they relate.[2]

Directive 2009/28/EC of the European Parliament and of the Council of 23 April 2009 on the promotion of the use of energy from renewable sources and the subsequent amendment of Directive 2001/77/EC and Directive 2003/30/EC introduced an obligation to establish a system of Guarantees of Origin and specifically for the purpose of publishing data on the primary energy source as referred to in Directive 2009/72/EC of the European Parliament and of the Council of 13 July 2009 on common rules for the internal market in electricity repealing Directive 2003/54 / EC.[3]

The regulatory framework for the implementation of the guarantees of origin system is defined by the Energy Act (Official Gazette 120/12, 14/14, 102/15), which stipulates that an energy origin guarantee system is introduced to end customers for the purpose of proving the share of energy produced from individual energy sources.

Guarantees of Origin is an electronic document for the purpose of proving the origin of energy to the customer in such a way that a certain share of electricity used for its consumption is produced from a specific primary energy source and should be the standardized size of 1 MWh. A GO shall be issued either for electricity produced from a plant using a renewable energy source or from a high-efficiency cogeneration plant, exclusively at the request of a privileged producer. Eligible manufacturers for incentive system installations entitled to an incentive price are not entitled to participate in the GO system.[3]

For the purposes of the RES Directive, energy from renewable sources is defined as "energy from renewable non-fossil sources, namely wind, solar, aerothermal, geothermal, hydrothermal and ocean energy, hydropower, biomass, landfill gas, sewage treatment plant gas and biogases".

The RES Directive requires the Member States to give producers the opportunity to obtain electronic GOs for energy generated from these sources. The Member States shall as such issue GOs for electricity, gas (including hydrogen) and heating and cooling. Article 19 of the existing Renewable Energy Directive states that each GO should contain information including but not limited to:

- Energy source;
- Start and end dates of production;
- Generator identity, location, type, date of operation, and capacity;
- Whether the GO relates to electricity or heating or cooling;
- Whether the installation benefits from state support;
- Date and country of issue; and
- Unique identification number.

There is no fixed price for a GO, and their value depends on market demand.

III. Organization of the Auction of Guarantees of origin in Croatia

In accordance with the Law on Renewable Energy Sources and High-Efficiency Cogeneration, HROTE, as the head of the ECO balance group consisting of eligible electricity producers for which the electricity purchase agreement is in force from the beginning of 2019, started selling 30% of electricity on the electricity market through CROPEX trading platform.[5]

With the transition of HROTE to the market sale of electricity, the possibility of establishing a system of selling GOs of electricity on a market basis has opened, precisely for electricity produced by eligible producers in the incentive system. Namely, GOs for the production of electricity from the plants in question can be issued within the Croatian Register of Guarantees of Origin and sold according to market principles, i.e., through auctions of GOs. During 2019, HROTE issued GOs for 30% of the electricity of eligible producers in the incentive system sold on the electricity market through the ECO balance group, which were then sold on the market through auctions of GOs, i.e., through CROPEX's auction system.[5]

After the conclusion of the auction and successful purchase and sale of GOs, the collected funds are transferred to the incentive system fund, while on the other hand sold GOs at auctions are transferred from HROTE's account in the Croatian Registry of Guarantees of Origin to the user accounts which buy GOs. For 2019, the percentage or share of electricity of eligible producers in the incentive system sold was 30% or 899,199 GOs. On the other hand, in 2020, the percentage or share of electricity of eligible producers in the incentive system sold was 60%, i.e., a total of 1,546,305 GOs and in 2021 2,030,603 GOs. [5]

Based on metering data from the billing metering point of the production plant, i.e., the control metering point of the production unit of the eligible producer in the incentive system obtained from the transmission system operator and the distribution system operator, HROTE determines the number of GOs be sold at auctions. HROTE also determines the minimum price of the GO offered at the auction for each individual auction. HROTE and CROPEX are obliged to publish on their websites the specification, date and time of the auction.[1]

The list of GOs auctions organized on CROPEX auction platform in 2020 and 2021 are shown in Tables 2 and 3.

Marko Kelava, Martina Vajdić, Boris Dokmanović, The progression of Guarantees of Origin trading in Croatia amidst the European framework, Journal of Energy, vol. 71 Number 4 (2022), 16–22
https://doi.org/10.37798/2022714457

TABLE I.

REGISTER OF GOS IN CROATIA

The registry of Guarantees of Origin (GO): period 1/1/2020-31/12/2020						
Registry activation date	Account holder	Name of account	Address of the account holder	Account holder's code	Account holder's role	The total sum of all transactions GOs on account holder's account in the period 1/1/2020-31/12/2020 (MWh)
21.4.2015.	HEP-Opskrba d.o.o.	643002406600047167	Ulica grada Vukovara 37, ZG	40XX20FR6K	Supplier	5.347.762
21.5.2015.	GEN-I Zagreb d.o.o.	643002406600047716	Radnička cesta 54, ZG	40XY21WN4S	Supplier	16.991
17.8.2015.	Proenergy d.o.o.	643002406600048058	Ulica grada Vukovara 284, ZG	40XL24ST6Q	Supplier	0
20.10.2015.	E.ON ENERGIJA d.o.o.	643002406600048232	Capraška ulica 6, ZG	40XR74MD2Y	Supplier	48.693
27.10.2015.	HEP-Proizvodnja d.o.o.	643002406600048317	Ulica grada Vukovara 37, ZG	40XY25GQ1X	Producer	9.616.786
21.3.2016.	CRODUX PLIN d.o.o.	643002406600049215	Savska Opatovina 36, ZG	40XT29EQ0M	Supplier	198
17.3.2017.	ADRIA WIND POWER d.o.o.	643002406600050990	Varaždinska 61, Sesvete	40XH60AR5M	Producer	10.080
30.11.2018.	VJETROELEKTRANA TRTAR-KRTOLIN d.o.o.	643002406600052567	Bože Pericica 30, Šibenik	40XZ08FJ62	Producer	55.736
22.01.2019.	ZAGREBAČKI HOLDING d.o.o.	643002406600052703	Ulica grada Vukovara 41, ZG	40XK72RM8Y	Producer	40.278
25.01.2019.	HIDRO-WATT d.o.o.	643002406600052710	Ožujska 21, ZG	40XD27KM6C	Producer	7.835
28.08.2019.	HEP d.d.	643002406600062627*	Ulica grada Vukovara 37, ZG	40XH57YZ3L	Trader	56.980
23.12.2019.	PETROL d.o.o.	643002406600063051*	Oreškovićeva 6/h, ZG	40XN18BC4D	Supplier	15.396
28.02.2020.	ENERGIA GAS AND POWER d.o.o.	643002406600063426*	Ulica Alexandera von Humboldta 4 B, ZG	40XZ59SA7C	Supplier	211.900
04.03.2020.	ENERGY SUPPLY EOOD	/	Grafa Ignatijeva 2, BUGARSKA	40XF26BZ8W	Trader	0
16.03.2020.	HOPS d.o.o.	643002406600063563*	Kupska 4, ZG	40XB91KC76	Supplier	183.790
18.05.2020.	Terremoto Energo-Projekt d.o.o.	643002406600063778*	Goricanska 23, ZG	40XK38XC62	Trader	178.928

TABLE II.

LIST OF GOS AUCTIONS IN 2020 [6]

List of auctions in 2020	Auction type	Auction date	GOs sold	Price EUR/GO
Production from Q4/2019	WIND	2020-01-21	274,482	0.36
Production January-February 2020	BIOMASS	2020-03-16	69,227	1.11
Production January-February 2020 (Comm. date 12-2015 to 12-2019)	WIND	2020-03-16	102,029	1.01
Production January-February 2020 (Comm. date 12-2009 to 12-2014)	WIND	2020-03-16	125,092	0.20
Production March-April 2020	BIOMASS	2020-05-20	64,486	1.50
Production March-April 2020 (Comm. date 12-2015 to 12-2019)	WIND	2020-05-20	147,806	1.21
Production March-April 2020 (Comm. date 12-2009 to 12-2014)	WIND	2020-05-20	143,961	0.17
Production May-June 2020 (Comm. date 06-2015 to 05-2020)	BIOMASS	2020-07-21	73,197	1.52
Production H1/2020 (Comm. date 09-2010 to 05-2014)	BIOMASS	2020-07-21	6,351	0.14
Production May-June 2020 (Comm. date 12-2015 to 12-2019)	WIND	2020-07-21	142,823	0.86
Production May-June 2020 (Comm. date 12-2009 to 12-2014)	WIND	2020-07-21	97,861	0.16
Production July-August 2020 (Comm. date 06-2015 to 08-2020)	BIOMASS	2020-09-18	65,175	1.35
Production July-August 2020 (Comm. date 12-2009 to 12-2014)	WIND	2020-09-18	73,893	0.12
Production July-August 2020 (Comm. date 12-2015 to 05-2020)	WIND	2020-09-18	135,855	1.11
Production September-October 2020 (Comm. date 06-2015 to 08-2020) - inst. cap. < 5 MW	BIOMASS	2020-11-19	43,850	1.61
Production September-October 2020 (Comm. date 12-2015 to 09-2020) - inst. cap. ≥ 5 MW	BIOMASS	2020-11-19	30,468	0.81
Production September-October 2020 (Comm. date 12-2009 to 12-2014)	WIND	2020-11-19	91,791	0.16
Production September-October 2020 (Comm. date 12-2015 to 05-2020)	WIND	2020-11-19	132,440	0.86

Table III.

List of GOs auctions in 2021 [6]

List of auctions in 2021	Auction type	Auction date	GOs sold	Price EUR/GO
Production H1/2020 (Comm. date 09-2011 to 05-2014)	BIOMASS	2021-01-21	2.574	0,25
Production November-December 2020 (Comm. date 06-2015 to 08-2020) - inst. cap. < 5 MW	BIOMASS	2021-01-21	50.012	1,56
Production November-December 2020 (Comm. date 12-2015 to 09-2020) - inst. cap. ≥ 5 MW	BIOMASS	2021-01-21	33.244	0,55
Production November-December 2020 (Comm. date 12-2015 to 05-2020)	WIND	2021-01-21	174.625	0,65
Production November-December 2020 (Comm. date 12-2010 to 12-2014)	WIND	2021-01-21	100.495	0,09
Production January-February 2021 (Comm. date 06-2015 to 08-2020) - inst. cap. < 5 MW	BIOMASS	2021-03-19	48.108	1,90
Production January-February 2021 (Comm. date 12-2015 to 09-2020) - inst. cap. ≥ 5 MW	BIOMASS	2021-03-19	32.444	0,17
Production January-February 2021 (Comm. date 12-2015 to 05-2020)	WIND	2021-03-19	195.330	0,21
Production January-February 2021 (Comm. date 12-2010 to 12-2014)	WIND	2021-03-19	115.080	0,20
Production March 2021 (Comm. date 06-2015 to 08-2020) - inst. cap. < 5 MW	BIOMASS	2021-04-21	24.961	2,11
Production March 2021 (Comm. date 12-2015 to 09-2020) - inst. cap. ≥ 5 MW	BIOMASS	2021-04-21	15.400	0,28
Production March 2021 (Comm. date 12-2015 to 05-2020)	WIND	2021-04-21	103.100	0,27
Production March 2021 (Comm. date 08-2011 to 12-2014)	WIND	2021-04-21	61.091	0,22
Production April 2021 (Comm. date 06-2015 to 08-2020) - inst. cap. < 5 MW	BIOMASS	2021-05-19	23.394	2,38
Production April 2021 (Comm. date 12-2015 to 09-2020) - inst. cap. ≥ 5 MW	BIOMASS	2021-05-19	16.771	0,51
Production April 2021 (Comm. date 12-2015 to 05-2020)	WIND	2021-05-19	88.006	0,51
Production April 2021 (Comm. date 01-2012 to 12-2014)	WIND	2021-05-19	53.377	0,47
Production May and June 2021 (Comm. date 06-2015 to 05-2021) - inst. cap. < 5 MW	BIOMASS	2021-07-22	48.103	3,25
Production May and June 2021 (Comm. date 12-2015 to 09-2020) - inst. cap. ≥ 5 MW	BIOMASS	2021-07-22	33.796	0,45
Production May and June 2021 (Comm. date 12-2015 to 05-2020)	WIND	2021-07-22	113.363	0,49
Production May and June 2021 (Comm. date 12-2010 to 12-2014)	WIND	2021-07-22	71.789	0,43
Production July and August 2021 (Comm. date 06-2015 to 05-2021) - inst. cap. < 5 MW	BIOMASS	2021-09-22	54.405	2,76
Production July and August 2021 (Comm. date 12-2015 to 07-2021) - inst. cap. ≥ 5 MW	BIOMASS	2021-09-22	32.160	0,76
Production July and August 2021 (Comm. date 12-2015 to 05-2020)	WIND	2021-09-22	134.540	0,78
Production July and August 2021 (Comm. date 02-2012 to 12-2014)	WIND	2021-09-22	59.406	0,78
Production September and October 2021 (Comm. date 06-2015 to 05-2021) - inst. cap. < 5 MW	BIOMASS	2021-11-23	57.958	2,21
Production September and October 2021 (Comm. date 12-2015 to 07-2021) - inst. cap. ≥ 5 MW	BIOMASS	2021-11-23	40.160	0,58
Production September and October 2021 (Comm. date 12-2015 to 05-2020)	WIND	2021-11-23	187.222	0,70
Production September and October 2021 (Comm. date 02-2012 to 12-2014)	WIND	2021-11-23	62.263	0,67

Marko Kelava, Martina Vajdić, Boris Dokmanović, The progression of Guarantees of Origin trading in Croatia amidst the European framework, Journal of Energy, vol. 71 Number 4 (2022), 16–22
https://doi.org/10.37798/2022714457

3.1 Croatian GOs Auction Results

In this chapter, the results of GOs auctions organized by HROTE and CROPEX depending on the source of energy, wind or biomass are shown. Results of GO auctions are divided depending on the commissioning date, while the results for biomass are additionally analyzed dependent on the installed capacity.

3.1.1 Auctions organized in 2020

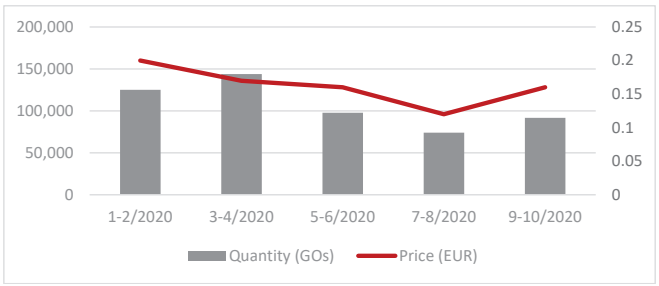

Fig. 1. Wind - commissioning date 2009-2014

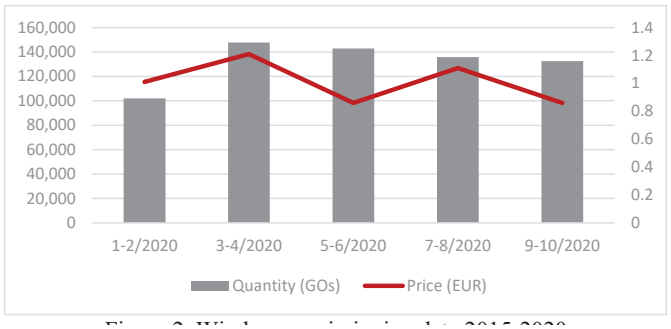

Fig. 2. Wind - commissioning date 2015-2020

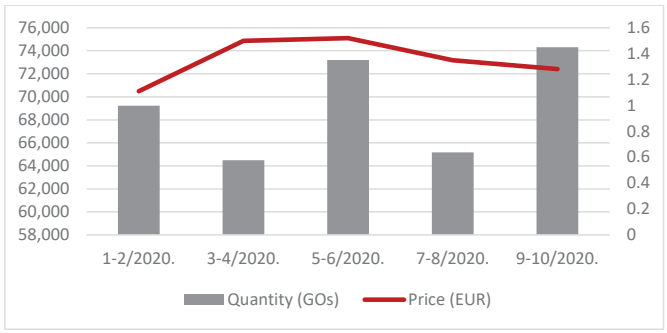

Fig. 3. Biomass - commissioning date 2015-2020

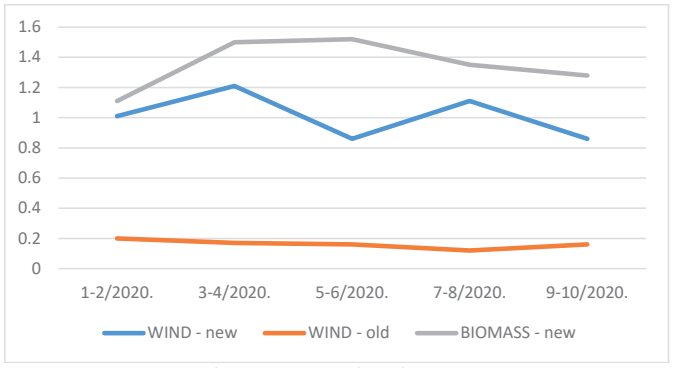

Fig. 4. GO prices in 2020

3.1.2 Auctions organized in 2021

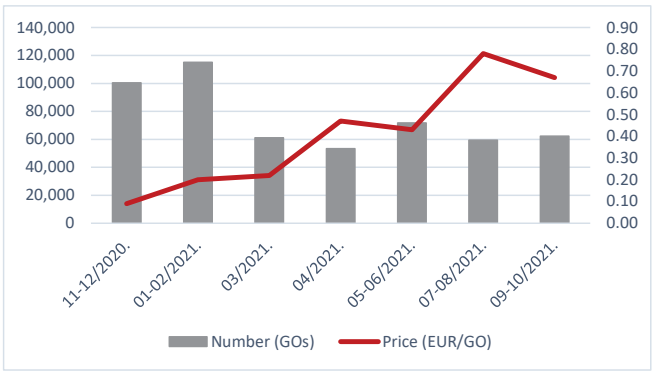

Fig. 5. Wind - commissioning date 2010-2014

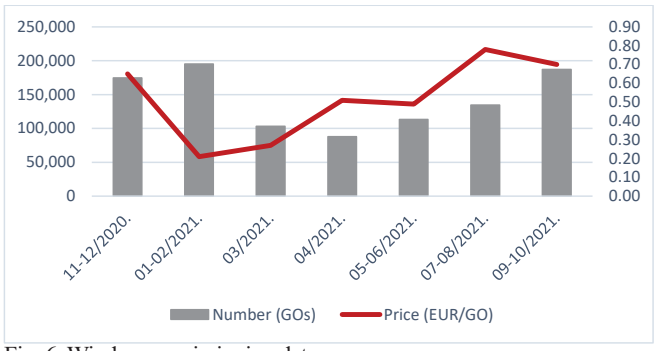

Fig. 6. Wind - commissioning date 2015-2020

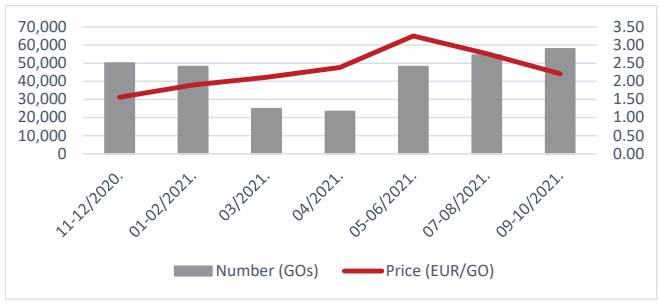

Fig. 7. Biomass - installed capacity <5MW; commissioning date 2015-2021

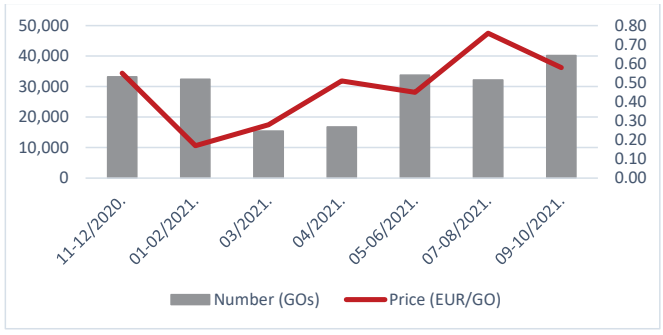

Fig. 8. Biomass - installed capacity >=5MW; commissioning date 2015-2021

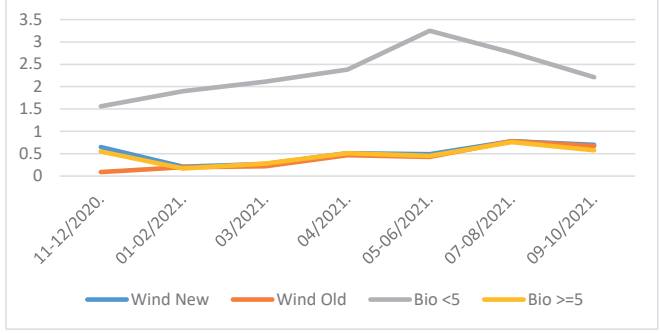

Fig. 9. GO prices in 2021

Marko Kelava, Martina Vajdić, Boris Dokmanović, The progression of Guarantees of Origin trading in Croatia amidst the European framework, Journal of Energy, vol. 71 Number 4 (2022), 16–22
https://doi.org/10.37798/2022714457

IV. Analysis of the Uk Guarantees of Origin Impacted by Brexit

In the United Kingdom (UK) Guarantees of Origin certificates are known as REGOs (Renewable Energy Guarantees of Origin). UK energy regulator Ofgem (Office of gas and electricity market) issues one REGO certificate per megawatt-hour (MWh) of eligible renewable output to generators of renewable electricity.

In line with the activities of BREXIT, which started from 1st of February 2020, The European Commission (EC) has stated that from 1st January 2021 onwards REGOs will no longer be recognized by the EU Member States. Based on the EDC statistics, it appears EU countries have already acted to reduce their import of REGOs prior to the end of the Brexit transition period. On the contrary, Ofgem has stated that they will still be accepting GOs from the EU Member States, which will enable UK electricity suppliers to continue to use them in order to comply with their fuel mix disclosure obligations, which requires licensed electricity suppliers to disclose to potential and existing customers the mix of fuels used to generate the electricity supplied. This has to be done by the 1st July of each year. The indication is that in the long-term, recognition of GOs from the EU Member States will continue only on a reciprocal basis.

REGO auctions are organized by e-POWER, on a quarterly basis. According to e-POWER, prices seem to be on an upward trend, with an increasing number of REGOs required to support more domestic and business green electricity tariffs as well as large corporates using REGOs as part of their ESG (environmental, social and governance impacts) reporting. In the last auction, 15 active bidders bid with over 3,500 bids.

Table IV.

e-POWER REGO Auction Results [7]

e-REGO track record

Auction Date	Biogas	MIW	Landfill	Biomass	Hydro	Wind	PV	Notes
09-Dec-21	£ 4.25	n/a	£ 4.27	£ 4.97	n/a	£ 6.17	£ 6.20	
08-Oct-21	£ 2.10	£ 2.10	n/a	£ 2.05	£ 3.00	£ 2.94	£ 3.00	Apr 21 Certificates onwards
06-May-21	£ 0.09	n/a	£ 0.03	£ 0.08	£ 0.70	£ 0.72	£ 0.70	Apr 20 to Mar 21 Certificates
09-Feb-21	£ -	MIW	£ 0.06	£ 0.05	£ 0.16	£ 0.16	£ 0.16	Notes
08-Oct-20	n/a	n/a	£ 0.06	£ 0.06	n/a	£ 0.14	£ 0.15	
16-Jul-20	n/a	n/a	£ 0.12	£ 0.10	£ 0.19	£ 0.22	£ 0.07	Apr 20 to June 2020 Certificates
05-May-20	n/a	n/a	n/a	n/a	£ 0.10	£ 0.05	£ 0.08	CP18
11-Mar-20	n/a	n/a	n/a	n/a	£ 0.15	£ 0.17	n/a	
30-Jan-20	n/a	n/a	n/a	£ 0.15	£ 0.28	£ 0.26	£ 0.30	
10-Sep-19	£ 0.40	£ 0.53	£ 0.51	£ 0.51	£ 0.50	£ 0.58	£ 0.62	
23-May-19	£ 0.22	n/a	n/a	£ 0.17	£ 0.28	£ 0.22	£ 0.23	

REGOs relating to Compliance Period 19 (April 2020 to March 2021) across all technologies were sold in the auction, but huge demand for "Deep Green" certificates (certifying solar PV, hydro and wind generation) pushed prices up to well over double the current market rates, and up fourfold on the last auction. The auctions helped to deepen the market for REGOs, increasing their value for renewable energy generators.[8]

While UK GOs have effectively been ruled out for usage in the EU, the effect on the overall EU market is expected to be minimal given the small volume exported from the UK. In the interim, while EU GOs are still valid for use in the UK, there is expected to be some administrative burden for traders. However, large changes in activity or prices are unexpected due to Brexit with current arrangements.[9]

V. GOs Price Overview across the Europe

Because the supply of renewable energy has tended to outstrip demand, average prices for European GOs have been relatively low, compared to power prices. During the summer of 2021, prices were quoted around an average of 0.45 EUR/GO for energy generated in 2021 from the main product groups of hydro, wind, solar, and biomass. However, strong market activity in September 2021 has seen these prices almost double, with prices for 2022 and 2023 generation quoted at twice as much – around 1.30 EUR/GO. At present, the GO market is not very transparent, with very little public exchange trading. Most contracts and prices remain private between the parties involved. The most publicly available prices for European GOs come from national auctions set up to sell GOs on behalf of countries that do not issue them to producers who benefit from public support schemes.[10]

However, these prices do not tell the whole story. Some specific GO products sell for up to 10 times the prices seen above. The market for Dutch wind is often noted as being one of the most competitive – Dutch wind was quoted at 2.70 EUR/GO in July 2021 for 2021 supply. The Dutch national rail company has an entirely electric fleet powered by local renewables and coupled with strong local demand from other Dutch consumers, GOs for Dutch wind tend to trade at significantly higher prices than the rest of the market. The value of other GOs, such as those included in PPAs or in domestic renewable electricity offers, may be higher or lower and may not be specified separately from the total cost of each MWh of renewable electricity, i.e., power price + GO price. In general, GO prices will rise in Europe as renewable energy demand catches up with GO supply.[10]

In 2021, unlike in 2020, it can be noticed that there is almost no difference in wind GOs price between GOs from 'old' and 'new' power plants (comm. date before and after 2015). Furthermore, it is noticeable that the only thing that remained the same is a significant difference between 'combo' GOs (small biomass <5 MW) from all other GOs. The reason for this does not lie in Brexit. The

Marko Kelava, Martina Vajdić, Boris Dokmanović, The progression of Guarantees of Origin trading in Croatia amidst the European framework, Journal of Energy, vol. 71 Number 4 (2022), 16–22
https://doi.org/10.37798/2022714457

value of the new power plants >5MW depends on the contract for differences (CFD) value in the United Kingdom (UK). Currently, the power prices are very high and thus the value of those GOs has decreased significantly. The new power plants <5MW are eligible for CFD and FIT exemption at the same time – thus their value is less affected by the lower power prices. The GOs of "new" power plants can be used in the UK by electricity suppliers to offset payments related to CfD levelisation (it's a green subsidy), so until recently, they were bidding at a premium for these GOs. Given that the participants in the auctions of guarantees of origin organized by HROTE and CROPEX come from different European countries, this explains that the price movement of GO at CROPEX is closely related to the price movement in the UK. Separation of auctions depending on the technology, age and installed capacity of the plant has so far proved to be a very good solution that makes it easier for auction participants to obtain a certain certificate (GO) at the desired price.

References

[1] Rules on conducting auctions of guarantees of origin of electricity, available at the link: https://www.cropex.hr/hr/dokumenti.html

[2] AIB, Guaranteeing the Origin of European Energy, available at: https://www.aib-net.org/

[3] Register of guarantees of origin, available at the link: http://www.hrote.hr/registar-jamstava-podrijetla

[4] System of guarantees of origin, available at the link: http://www.hrote.hr/sustav-jamstava-podrijetla

[5] Annual Report on the Guarantee of Origin System in the Republic of Croatia for 2019, available at the link: http://www.hrote.hr/izvjestaji-310

[6] Available at the link: https://www.cropex.hr/hr/obavijesti.html

[7] e-POWER results, available at the link: http://www.epower.net/downloads/e-REGO_Track_Record_20211214.pdf

[8] Available at the link: https://www.spglobal.com/platts/en/market-insights/latest-news/electric-power/051121-dark-green-rego-prices-rocket-in-latest-uk-electronic-auction

[9] Available at the link: https://www.greenfact.com/News/1356/Brexit-and-the-effect-on-the-GO-market

[10] Guarantees of Origin and Corporate Procurement Options, available at: https://resource-platform.eu/wp-content/uploads/Guarantees-of-Origin-and-Corporate-Procurement-Options.pdf

Journal of Energy

VOLUME 71 Number 4 | 2022

journal homepage: http://journalofenergy.com/

Corrosion Detection and Surface Repair with Coatings on Condensate Storage Tanks Internal Surfaces

Matija Gulič, Sanja Smirić, Lenart Pušnik

***Summary* —In the Nuclear power plant Krško, there are two single hull condensate storage tanks with floating diaphragm each containing up to 757 m³ of demineralized water. The main purpose of these two storage tanks is to provide a capacity of cooling water for cooling the reactor coolant system via steam generators with the use of auxiliary feedwater pumps. This is a very important function from the safety point of view and that is the reason that both storage tanks are listed as safety class 3 components. It is also possible to fill up the condensate system if other means are not available. Condensate storage tanks are subject to periodic testing and periodic inspections to determine the condition of the components. Both tanks are in operation since the start-up of the powerplant, are located outside, and are exposed to different degradation processes. There was a concern that the tanks are leaking because there were often small puddles of water near the tanks. There were no changes in the levels of tanks. The design of tanks is a single hull, so there is no indication if a small leak is present. In the outage 2018, both tanks were emptied and examined with NDE methods to find any corrosion damage of bottom plates and any untight spots on adjacent welds. The article is about the NDE methods that were used (Magnetic Flux Leakage, Ultrasonic and Vacuum Box inspection) to determine the condition of the floor plates and adjacent welds as well as the process of internal surface reparation with coatings. Process of coatings qualification for use in safety class components is also explained: dedication process for material up-grade from non-safety related to safety-related because CY tank linings are classified as safety-related according to RG 1.54, rev 2 and corresponding ASTM standards and NEK technical specification SP-A5001. All activities for surface repair with coatings shall comply with safety-related requirements. Also, extensive immersion tests with selected and specially defined parameters were performed in NEK chemical laboratory in order to select the most suitable coating system for surface repair of CY tank floor lining. Further details concerning immersion tests are presented below.**

***Keywords* — Corrosion, Condensate Tank, NDE, Coating, Aging Management**

I. Introduction

In the Nuclear power plant Krško, there are two single hull condensate storage tanks with floating diaphragms each containing up to 757 m³ of demineralized water. They are designated as CY101TNK-001 and CY101TNK-002 respectively (Figure 1). The main purpose of these two storage tanks is to provide a capacity of cooling water for cooling the reactor coolant system via the auxiliary feedwater system. When needed, the water from the condensate storage tanks is pumped with two motor-driven pumps or one steam-driven auxiliary feedwater pump in two steam generators to cool down steam generators. This is a very important function from the safety point of view and that is the reason that both storage tanks are listed as safety class 3 components. The diameter of each tank is 10,6 m with a height of 9,5 m, the nominal thickness of bottom plates is 9 mm and the nominal thickness of shell plates is 15 mm. The material of the plates is carbon steel, which is susceptible to corrosion if it is not treated properly with the coatings. Both tanks are in operation since the start-up of the powerplant, are located outside, and are exposed to influence of the environment. Long-term exposure to environmental conditions can result in a build-up of different degradation mechanisms. Due to the combination of carbon steel and environmental conditions, different forms of corrosion are expected to occur through the lifetime of the components. Condensate storage tanks are subject to periodic testing and periodic inspections to determine the condition of the components. Tanks are monitored through the following plant programs: ADP-1.4.235; Preventive maintenance program for secondary side stabile equipment, TD-2ZZ; aging management program - Above grounds metallic tanks program [1] and TD-A21; aging management program - Internal coatings/linings for in-scope piping, piping components, heat exchangers and tanks [2]. The first program is more operational related, while the other two programs are oriented more toward long-term operation and for managing potential degradation mechanisms.

Fig. 1. Condensate storage tanks 1 and 2

(Corresponding author: Matija Gulič)

Matija Gulič, Sanja Smirić and Lenart Pušnik are with the Nuklearna elektrarna Krško (NEK)Krško, Slovenia (e-mails: matija.gulis@nek.si, sanja.smiric@nek.si, lenart.pusnik@nek.si)

Matija Gulič, Sanja Smirić, Lenart Pušnik, Corrosion Detection and Surface Repair with Coatings on Condensate Storage Tanks Internal Surfaces, Journal of Energy, vol. 71 Number 4 (2022), 23–29
https://doi.org/10.37798/2022714412

Fig. 2: Possible signs of leakage on tank 1

There was a concern that the tanks are leaking because there were often small puddles of water nearby the tanks (Figure 2) although there were no measurable changes in the levels of tanks. The tanks are designed as a single hull construction, so there is no indication if a small leak is present. The first concern, that there might be some leaks present on tank no.1 was reported through the Corrective Action Program (CAP) already in 2013 [3]. The following inspection in 2013 was a visual inspection with the addition of ultrasonic (UT) thickness measurement by the 25 cm grid and did not find any deviations from the normal state of the component. Concern for degradation of bottom steel plates was still present, because of the scarcity of the UT thickness measurements. For the following outage in 2016 draining of both tanks was not planned, so only during the outage 2018 complete inspection was possible.

In the outage 2018, both tanks were emptied and examined with Non-Destructive Examination (NDE) methods to find any corrosion damage to bottom plates and to locate any untight spots on adjacent welds [4]. Magnetic Flux Leakage (MFL) was recognized as the most suitable NDT method for the detection of any deviations of the bottom plates thickness due to the corrosion. With this technique, the full coverage was obtained and not only spot measurements as in the 2013 UT inspection. Ultrasonic – UT inspection was still used for interpretation and exact measurement of indications obtained with the MFL technique.

With the UT measurements, on some locations, it's been confirmed that the thickness of bottom plates is less than 50% of the nominal plate thickness ($t_{meas}<t_{nom}$). Nominal thickness is t_{nom}=9mm and measured thickness are t_{meas}=4mm and t_{meas}=2mm).

Corrective actions were taken in a form of welded steel patches on affected areas where $t_{meas}<t_{nom}$. Before coating, steel patches welds were tested with the Vacuum Box technique for tightness.

As for the finish, treatment of repaired surfaces was performed with the use of qualified coatings for such application, because CY tank linings are classified as safety-related according to Regulatory Guide 1.54, rev. 2 [5], corresponding ASTM standards and NEK technical specification SP-A5001 [6]. For potential coatings, extensive immersion tests with selected and specially defined parameters were performed in NEK chemical laboratory to select the most suitable coating system for surface repair of CY tank lining and dedication process for material up-grade from non-safety related to safety-related.

II. Plant Specific Programs: TD-2ZZ And TD-A21

A. TD-2ZZ: Aboveground Metallic Tanks aging management program

This program [1] manages the effects of loss of material on the outer surfaces of above-ground tanks constructed on concrete or soil. This program credits the standard industry practice of coating or painting the external of steel tanks as a preventive measure to mitigate corrosion.

The program relies on periodic inspections of metallic tanks (with or without coatings) to manage the effects of corrosion on the intended function of these tanks. Because lower portions of the tank are on concrete or soil, corrosion may occur at inaccessible locations. Visual inspections cover the entire outer accessible surface of the tank and inaccessible outer surfaces are inspected by UT and MFL from inside when tank is empty.

Accordingly, verification of the effectiveness of the program is performed to ensure that significant degradation in inaccessible locations is not occurring and that the component intended function is maintained during the period of extended operation.

The scope of the TD-2ZZ program are CY101TNK-001 and CY101TNK-002 (condensate system) and DO100TNK-003 (diesel oil system).

This program utilizes periodic plant inspections to monitor the degradation of coatings, sealants, and caulking because it is a condition directly related to the potential loss of materials. Additionally, thickness measurements of the bottoms of the tanks are made periodically for the tanks monitored by this program as an additional measure to ensure that the loss of material is not occurring at locations that are inaccessible for inspection.

Degradation of an exterior metallic surface can occur in the presence of moisture; therefore, an inspection of the coating is performed to ensure that the surface is protected from moisture. Conducting periodic visual inspections at each outage to confirm that the paint, coating, sealant, and caulking are intact is an effective method to manage the effects of corrosion on the external surface of the component except the inaccessible outer surfaces. Potential corrosion of tank bottoms is determined by taking non-destructive examination methods shown in Table 1.

Table 1

Inspection scope for program TD-2ZZ

Tank label	Examination method	Scope	Frequency
CY101TNK-001 and 002	Visual examination	External surface	1 per year
CY101TNK-001 and 002	*UT and *MFL	Bottom thickness	1 per 6 years
DO100TNK-003	Visual examination	External surface	1 per year

*(UT) ultrasonic testing thickness measurements

*(MFL) Magnetic flux leakage

The effects of corrosion of the inaccessible external surface are detectable by UT thickness measurement of the tank bottom and are monitored and trended if significant material loss is detected where multiple measurements are available.

Acceptance Criteria: Any degradation of paints or coatings (corrosion) is reported and requires further evaluation. Corrosion is unacceptable and needs to be evaluated using the corrective action

Matija Gulis, Sanja Smirić, Lenart Pušnik, Corrosion Detection and Surface Repair with Coatings on Condensate Storage Tanks Internal Surfaces, Journal of Energy, vol. 71 Number 4 (2022), 23–29
https://doi.org/10.37798/2022714412

program. UT thickness measurements of the tank bottom are evaluated against the design thickness and corrosion allowance. Any measurements of the tank bottom thickness smaller than 5.0 mm require further evaluation and repair.

Minimal tank bottom thickness criteria is determined in standard EEMUA Publication 159, Above Ground Flat Bottomed Storage Tanks: A Guide to Inspection Maintenance and Repair, Edition 5;

TD-A21: Internal coatings/linings for in-scope piping, piping components, heat exchangers and tanks [2]

This program includes internal coatings/linings that are permanently, temporary or in case of anticipated transient conditions immersed in various media: diverse water (closed-cycle cooling, raw, borated and waste water), fuel or lubricating oils and are safety-related - internal coatings/linings of in-scope piping, piping components, heat exchangers, and tanks exposed to closed-cycle cooling water, raw water, treated water, treated borated water, waste water, fuel oil, and lubricating oil where the loss of coating or lining integrity could prevent the satisfactory accomplishment of any of the SSC's (structures, systems, components) intended functions.

III. Monitoring, Testing and Inspection Activities

At the request of the Krško Nuclear Power Plant, the outside contracting company performed testing of both condensate storage water tanks CY101TNK-001 and CY101TNK-002. Inspections were performed due to requirements in the CAP [3].

After the tanks were drained and cleaned, the inspection was performed from the inside. The inspection includes:

1. Inspection of the bottom plates with MFL method, scope 100%
2. Inspection of the bottom plates with vacuum box method, scope 100%
3. Inspection of the bottom plate welds with vacuum box method, 100%
4. Inspection of the corner welded joins, with vacuum box method, 100%

A. Inspection methods

Magnetic Flux Leakage (MFL) Method

Magnetic flux leakage is an electromagnetic non-destructive testing technique used to detect corrosion and pitting. MFL method uses a powerful magnet to magnetize the conductive material under test. If any discontinuity exists in material like corrosion or material loss, the magnetic field "leaks" from the material.

MFL probes incorporate a magnetic detector placed between the poles of the magnet where it can detect the leakage field. The magnetic field induced in the material (plate) saturates it until it can no longer hold any more magnetic flux (Figure 3). The magnetic flux overflows and leaks out of the plate and strategically placed sensors can accurately measure the three-dimensional vector of the leakage field (Figure 4).

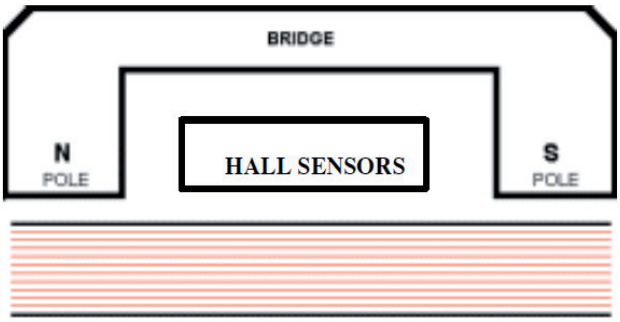

Fig. 3. Saturated material (plate)

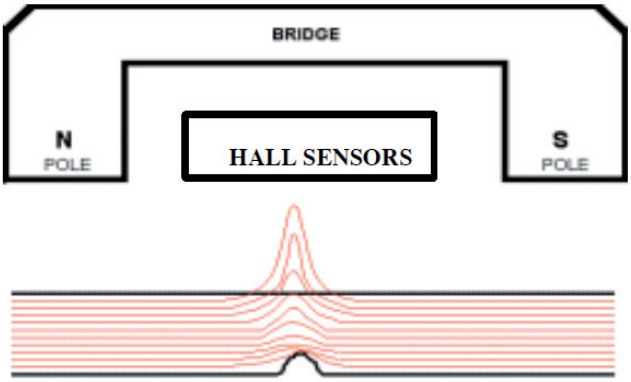

Fig. 4. Magnetic flux leaks from material

Fig. 5. Inspection of bottom plates using MFL detection scanner.

Inspection of the bottom plates with the MFL method (Figure 5) was performed due to the determination (identification) of pitting corrosion from underneath (bottom side of the plates).

Vacuum box testing method

Vacuum Box testing (Figure 6) is a non-destructive method used to check for any leaks or faults in the welding of the bottom

Matija Gulis, Sanja Smirić, Lenart Pušnik, Corrosion Detection and Surface Repair with Coatings on Condensate Storage Tanks Internal Surfaces, Journal of Energy, vol. 71 Number 4 (2022), 23–29
https://doi.org/10.37798/2022714412

& annular plates of the storage tank. The vacuum pump attached creates a vacuum in the vacuum box, which shows bubbles of the soap water applied to the weld in case of any leaks or faults present. This is one of the most adoptive test methods to detect leaks or defects and is widely used in the inspection of tanks. Inspection of the bottom plates and adjacent welds with the vacuum box method did not reveal any leaking points.

Fig. 6 Vacuum box inspection of welded patch

B. Inspection results

Visual inspection of the internal surface

Visual inspection confirmed that the internal coating of the tank plates and welds are in very good condition, without chipping, flaking, corrosion, or other damage present. The good condition was confirmed for the bottom surfaces as well as for the shell [4].

MFL Inspection

MFL inspection confirmed damage on the bottom plates from underneath (inaccessible side of the tanks) on both condensate storage tanks. In all locations where damage was detected, additional ultrasonic inspections were performed in order to perform the sizing of the located damage. All locations detected with MFL were confirmed with the ultrasonic inspection.

Two locations with corrosion damages were confirmed on the floor plates on condensate tank CY101TNK-001. Six locations with corrosion damage were confirmed on the lower part of floor plates and two locations with mechanical damage on the upper surface of floor plate on condensate tank CY101TNK-002 [4].

All damaged locations were repaired with welded patches and exanimated with the vacuum box method.

Vacuum box testing inspection

Inspection of the bottom plates with welded patches and adjacent welds with the vacuum box method did not reveal any damage that cause leakage on condensate tanks [4].

IV. Requirements for Surface Protection with Coating Materials

A. Service Level III Coatings

Internal surfaces of condensate storage tanks (internal coatings/linings) are according to Regulatory Guide 1.54, rev 2 "Service Level I, II, and III Protective Coatings Applied to Nuclear Power Plants", US NRC, 2010 [5], corresponding ASTM standards and NEK technical specification (SP-A5001 [6]) classified as Safety Related Service Level III coatings therefore specific requirements for safety-related items and/or services shall be implemented.

Coating Service Level III, as defined by [5], is a term used to describe areas outside Reactor Containment where coating failure could adversely affect the safety function of a Safety Related structure, system, or component (SSC). The selection of coating materials and performance of coating work for this service level should reflect immersion and such other service conditions as might be anticipated throughout the coatings service life expectancy. Specifically, coating work for the following structures and equipment is under Coating Service Level III: fuel pools and canals, if coated, and refueling water storage tanks or such other tanks constituting ECCS water sources.

B, Requirements for SL III Coatings

Special activities shall be performed before the application of protective coating systems to steel or any other internal/external surfaces or related coating work such as: Selection and Qualification of coating systems, Manufacturing, Preparation of substrates, Application of the coating system, Testing and Inspection Requirements, Personnel Qualification Requirements, Condition Assessment and Receipt and Storage of safety-related protective coating systems.

The coating/lining Supplier/Manufacturer shall provide products information and characteristics (in accordance with NACE TM0404): Product Data Sheet (PDS), Material Safety Data Sheet (MSDS), QA program, Coating Technology (ambient and material conditions, required surface preparation, application instructions, application and inspection procedures…), Qualification Test Reports, training program, qualification and certification of application personnel and inspectors.

C. Immersion Tests

Due to the safety-related nature of internal coatings/linings inside CY tanks and corresponded requirements for material selection and application several tests had to be performed before lining execution. Furthermore, CY tanks contain deionized water (Make-up water) which shall comply with specific chemical criteria listed in NEK procedure ADP 1.6.021 "Kemijske specifikacije in kriteriji za korektivno ukrepanje", ref.[7].

Table II

Chemical parameters for DD water in CY101TNK-001/002

Control parameter	Expected Value
Total conductivity at 25°C (µS/cm)	≤ 0.1
Dissolved oxygen (µg/kg)	≤ 100
Silicium (µg SiO_2/kg)	≤ 10
Diagnostic parameter	
Total organic carbon (µg/kg)	≤ 100
Hydrazine (µg/kg)	≥ 3 × [O_2]

Matija Gulis, Sanja Smirić, Lenart Pušnik, Corrosion Detection and Surface Repair with Coatings on Condensate Storage Tanks Internal Surfaces, Journal of Energy, vol. 71 Number 4 (2022), 23–29
https://doi.org/10.37798/2022714412

NEK performed specific immersion tests following the guidelines to best industrial practice for material selection. Tests were implemented according to NACE TM0174 Laboratory Methods for the Evaluation of Protective Coatings and Lining Materials on Metallic Substrates in Immersion Service, ref.[8] and ASTM D7230 Standard Guide for Evaluating Polymeric Lining Systems for Water Immersion in Coating Service Level III Safety-Related Applications on Metal Substrates[9]. Internal coatings/linings shall meet excellent physical and chemical properties required for the immersion environment and also no leaching of aggressive ions to the working medium shall occur (this may have a negative influence on NEK CPI – Chemistry Performance Indicator for secondary chemistry).

NEK selected several epoxy based coating systems for further immersion tests:

- Belzona 1391T (DFT 500 µm), BELZONA;
- Amercoat 90N (DFT 300 µm), PPG;
- Remoplast RA 122 (DFT 400 µm), REMBRANDTIN;
- Epolor Cargo HB B (DFT 400 µm), HELIOS and
- Hempadur 35560 (DFT 400 µm), HEMPEL.

For the purpose of testing materials all proposed/selected coating materials were applied on test coupons (carbon steel, dimensions 150×75×2.5 mm, 5 test coupons/system) in accordance with ASTM D5139 Standard Specification for Sample Preparation for Qualification Testing of Coatings to be Used in Nuclear Power Plants [10] (see Figure 7 and 8). Before material application, all coupons received surface preparation to grade Sa 2.5 according to ISO 8501-1.

Fig. 7. Test coupons Hempel

Fig. 8. Test coupons Belzona

Before immersion tests a final drying of coating on test coupons was accomplished at room temperature for a period at least of 3 days. Afterwards test coupons were visually examined due to local defects (in accordance with ISO 4628-1 to 5), the dry film thickness was measured, also the adhesion measurement was performed (pre and after immersion tests; in accordance with ASTM D4541 "pull-off test") and finally EIS (Electrochemical Impedance Spectroscopy) was determined (ISO 16773-1 to 4; requirement: no porosity – before/after immersion, Figure 9).

Fig. 9. Impedance measurement

Immersion tests (according to NACE TM 0174, procedure B [8]) lasted for 14 days and were performed in NEK chemical laboratory. Three (3) test coupons/coating systems were immersed in pure water (Q water) at a volume of 900 mL (Figure 10).

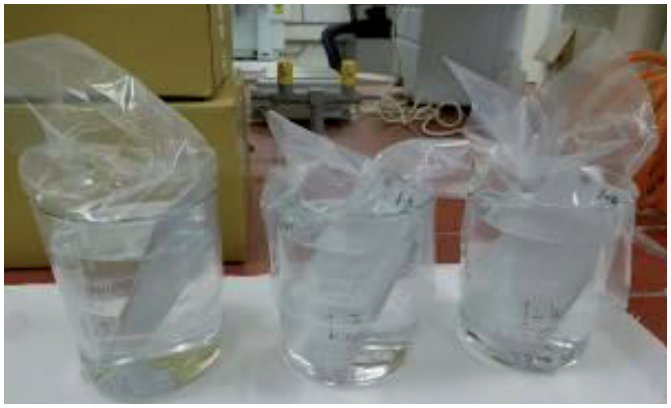

Fig. 10. Test coupons in immersion

Matija Gulis, Sanja Smirić, Lenart Pušnik, Corrosion Detection and Surface Repair with Coatings on Condensate Storage Tanks Internal Surfaces, Journal of Energy, vol. 71 Number 4 (2022), 23–29
https://doi.org/10.37798/2022714412

Fig. 11. Samples of working fluid in NEK laboratory

Samples of working fluid (water medium) were analyzed in the NEK chemical laboratory (Figure 11) to determine the presence of released anions (sulphates, chlorides, fluorides, acetates and formiates – in accordance with procedure CAP-6.552, Določevanje anionov z ionskim kromatografom ICS 3000, [11]) inside specified values defined in ADP-1.6.021, Kemijske specifikacije in kriteriji za korektivno ukrepanje [7]. Samples were analyzed before the beginning of immersion tests, after 7 days and at the end of immersion (14 days period).

$$\mathbf{c}_{\mathrm{ekv}} = \mathbf{c}_{\mathrm{meas}} \times \frac{A_{CY} \times V_{test}}{V_{CY} \times A_{coupon}}$$

c_{ekv} … concentration of water medium (in CY tank)

c_{meas} … measured concentration of testing water medium

A_{coupon} … immersed surface of test coupon (200 cm^2)

V_{CY} … volume of water medium in CY tank (700 m^3)

V_{test} … test water medium (900 ml)

Measured concentrations were considered in the equation stated above, so no c_{ekv} (concentration of water medium inside CY tank) was exceeded as stated in ADP-1.6.021[7].

The conclusion of immersion tests confirmed the most suitable coating materials for reparation of floor plates inside condensate storage tanks – Hempadur 35560 and Belzona 1391T. Belzona 1391T was selected because it had been already used in NEK as a Service Level III coating for surface reparation inside Component Cooling Heat Exchangers.

D. Dedication process

NEK performed the dedication process as a combination of the technical survey at manufacturer headquarter in the UK and verification of specific critical characteristics of purchased material. After successful completion of the technical survey, laboratory testing for critical characteristics was implemented by NEK in independent and accredited laboratories. NEK Nuclear Coating Specialist selected and defined critical characteristic for material verification such as determination of density and dry solids (in accordance with ISO 2811-1 and ISO 3251), determination of chemical composition by using a method of fingerprinting FTIR (Fourier Transform Infrared Spectroscopy) and also a verification of rheological properties of selected materials (rotational and oscillation tests were performed). All mentioned tests were performed on procured material batches. The extensive dedication process showed positive results in comparison with technical data sheets given by the manufacturer so NEK concluded that the dedication process was successfully completed and material could be used for intended safety related application.

E. Application of coating material on internal steel plates

In outage 2018 CY101TNK-002 was emptied so two (2) steel plates inside CY101TNK-002 were coated with coating material Belzona 1391T (working order 126432, Figure 12 and 13). The material application was performed in accordance with product data sheet (PDS) requirements. After drying of coating system several measurements were carried out: dry film thickness, adhesion testing, and solvent resistance rub [12]. It was confirmed that the coating is properly dried and applied before closing and filling the condensate storage tank.

Fig. 12. Steel plate inside CY tank

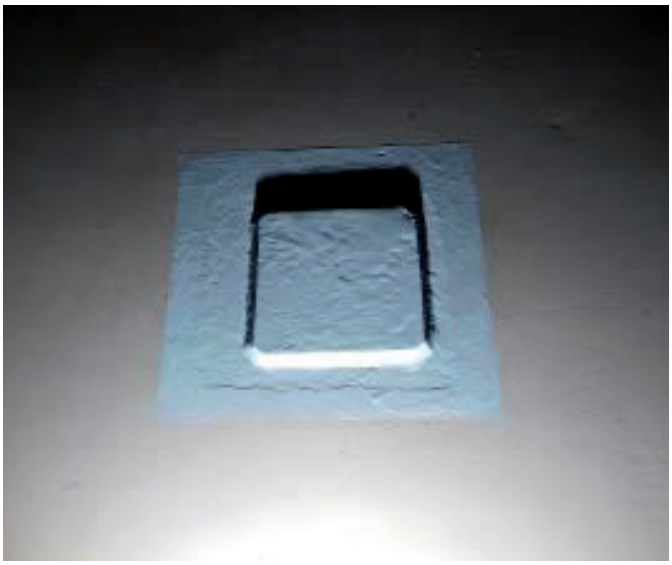

Fig. 13. Coated steel plate inside CY tank

During the next outage in 2021 seven (7) steel plates inside CY101TNK-001 were coated (work order 166115, Figure 14 and 15). All required activities were implemented to ensure the adequacy of execution of coating application (DFT and adhesion measurement, solvent rub test).

Matija Gulis, Sanja Smirić, Lenart Pušnik, Corrosion Detection and Surface Repair with Coatings on Condensate Storage Tanks Internal Surfaces, Journal of Energy, vol. 71 Number 4 (2022), 23–29
https://doi.org/10.37798/2022714412

Fig. 14. Steel plates inside CY tank

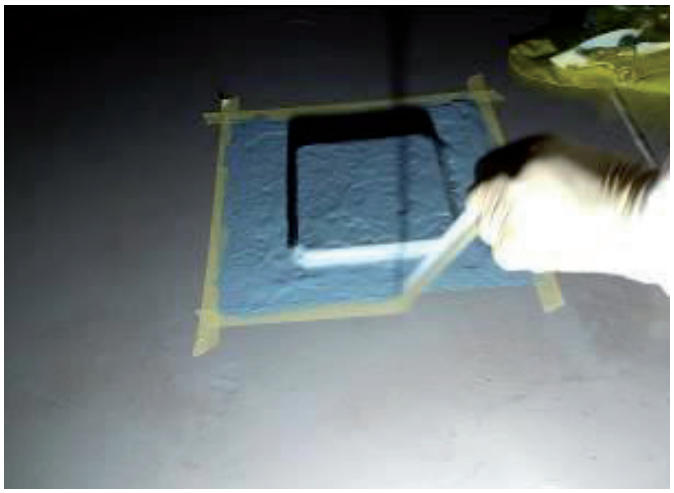

Fig. 15. Coated steel plate inside CY tank

V. Conclusion

The inspection of the condensate storage tanks is by the book example of managing the aging mechanisms in the NPP Krško [13]. The purpose of the aging management programs is to monitor components and to detect degradation before that degradation can cause the failure of the component. Periodically, the inspections are performed as per program requirements, but in this case, additional effort was taken due to the possibility of leaking and related CAP report [3].

The inspection did not reveal holes or degraded areas where leaking is possible, only indications of corrosion underneath the bottom plates at some locations. Corrective measures were taken in a form of welded patches, welds tested, and affected areas treated with the qualified coating. Performance of the job as a whole also presents a good practice of cooperation between organization structures within the NPP Krško for solving such a problem during an outage, when time and resources are limited due to a great number of other activities going on in the meantime. With that job done, NPP Krško has set up a benchmark for inspection and repair of single-hull holdup tanks.

References

[1] TD-2ZZ; Aboveground Metallic Tanks aging management program

[2] TD-A21; Internal coatings/linings for in-scope piping, piping components, heat exchangers and tanks

[3] NEK Corrective Action Program ZKP 2013-1727

[4] Final report of 2018 CY tanks inspection using NDE

[5] Regulatory Guide 1.54, rev 2 "Service Level I, II, and III Protective Coatings Applied to Nuclear Power Plants", US NRC, 2010

[6] SP-A5001, rev. 0, Service Level III Coatings

[7] ADP-1.6.021, Kemijske specifikacije in kriteriji za korektivno ukrepanje

[8] NACE TM0174 Laboratory Methods for the Evaluation of Protective Coatings and Lining Materials on Metallic Substrates in Immersion Service

[9] ASTM D7230 Standard Guide for Evaluating Polymeric Lining Systems for Water Immersion in Coating Service Level III Safety-Related Applications on Metal Substrates

[10] ASTM D5139 Standard Specification for Sample Preparation for Qualification Testing of Coatings to be Used in Nuclear Power Plants

[11] CAP-6.552, Določevanje anionov z ionskim kromatografom ICS 3000

[12] ASTM D5161, Standard Guide for Specifying Inspection Requirements for Coating and Lining Work (Metal Substrates)

[13] NUREG 1801 rev.2; Generic Aging Lessons Learned (GALL) Report

Journal of Energy
VOLUME 71 Number 4 | 2022
journal homepage: http://journalofenergy.com/

Characterization of the GBC-32 Fuel Assembly Source Terms

Mario Matijević, Matej Pekeč

Summary — **This paper presents burnup/depletion calculations of the typical Westinghouse 17x17 fuel assembly to be used as a radioactive waste package in a Generic Burnup Credit cask benchmark problem with 32 elements (GBC-32). This first phase is addressing spent fuel source terms calculation while evaluation of the shielding performance of the GBC-32 cask is planned for the second phase. The TRITON-NEWT methodology of the SCALE6.1.3 program package was used in a tandem with ORIGEN-S code for deterministic 2D calculation of the GBC-32 fuel assembly neutron multiplication factor, providing spatial-temporal fluxes and isotopic concentration change. The burnup simulation was done up to 60 GWd/tU with sensitivity analysis of relevant physical parameters influenced by the working cross-section library. This approach also allowed generation of the specific user-defined collapsed cross-section libraries as a function of fuel enrichment and burnup level. Calculation of isotopic concentrations, decay heat, neutron-gamma spectra and major actinides activity for different fuel assembly cooling periods was performed using ORIGEN-ARP module.**

Keywords — **SCALE, NEWT, TRITON, burnup, depletion**

I. Introduction

The Generic Burnup Credit cask (GBC-32) benchmark problem represents a real-life burnup credit style cask, preserving all important features through approximations, hence eliminating nonessential details and proprietary information [1]. The purpose of the GBC-32 benchmark is to provide a reference configuration for estimation of spent fuel (SF) reactivity margin available for fission products and minor actinides as a function of initial enrichment, burnup, and cooling time. Estimates of the additional reactivity margin for this reference configuration may be compared to a similar burnup-credit cask to provide an indication of the validity of specific design characteristics. A conservative approach to criticality safety analyses of commercial PWR fuel assembly (FA) storage and transport casks assumes the SF to be fresh or unirradiated, with isotopic concentrations defined by allowable enrichment [2]. This provides upper bounding value for reactivity, ignoring fuel operational history and simplifying analysis. However, this approach is lacking the decrease in reactivity of SF as a result of irradiation, giving conservative safety margin which limits cask capacity. A more realistic approach is including reduction in reactivity due to fuel burnup which is known as burnup credit. This will explicitly model reduction of fissile nuclides and the production of actinides and fission-product neutron absorbers. To provide a reference results for a burnup credit cask, resembling to a typical real-life configuration, a generic GBC-32 cask with 32 spent FAs was developed [1]. The reference results can be used to estimate additional reactivity margin coming from actinide nuclides and fission products. The essential part of criticality safety analyses is thus a detailed knowledge of FA geometry, initial material composition, operational history, and neutron-gamma source terms after cooling period.

This paper is presenting application of SCALE6.1.3 [3] transport theory codes for detailed isotopic analyses of an optimized Westinghouse 17x17 fuel assembly (OFA) in the framework of the GBC-32 benchmark. The performed TRITON [4] calculations quantified neutronic and isotopic characteristics of OFA by means of 2D deterministic transport theory code NEWT [3][5]. The depletion calculations of OFA were done in tandem with ORIGEN-S code up to a burnup of 60 GWd/tU using nominal power of 40 W/gU. Calculated k-eff values are provided as a function of burnup and cooling time for initial enrichments of 2 w/o, 3 w/o, 4 w/o, and 5 w/o of ^{235}U. The values are provided for burnup up to 60 GWd/tU with 20 time steps (75 days per step), and for cooling period up to 40 years (9 time steps). These TRITON-NEWT calculations coupled with ORIGEN-S also allowed generation of the specific user-defined collapsed cross-section libraries with 49 groups as a function of fuel enrichment and burnup level. Calculation of isotopic concentrations, decay heat, neutron-gamma spectra and major actinides activity for different fuel assembly cooling periods was performed using ORIGEN-ARP module [6]. These OFA results will be used as a starting point for the development of Monte Carlo (MC) GBC-32 cask model, which will be further analyzed with MAVRIC/Monaco shielding sequence of SCALE6.1.3 code package.

This paper is organized as follows. Chapter 2 gives basic description of an optimized 17x17 Westinghouse fuel assembly, which is used in the GBC-32 benchmark. The SCALE6.1.3 computational methods for deterministic 2D burnup/depletion of FA are presented in Chapter 3. The OFA TRITON model is given in Chapter 4. Chapter 5 gives TRITON-NEWT standalone results for OFA presenting method of generating weighted (collapsed) cross-section library with user defined 49 groups. The TRITON depletion calculations of OFA are presented in Chapter 6, together with ORIGEN-ARP results for neutron-gamma source terms. Discussion and conclusions are given in Chapter 7, while reference list is given at the end of the paper.

(Corresponding author: Mario Matijević)
Mario Matijević and Matej Pekeč are with the University of Zagreb Faculty of Electrical Engineering and Computing (FER)Zagreb, Croatia (e-mails: mario.matijevic@fer.hr, matej.pekec@fer.hr).

II. Optimized Fuel Assembly in GBC-32 Cask

The burnup credit can increase storage and transport cask capacities by 1/3, so for a standard rail-type cask this means increase from 24 to 32 FAs for large PWR assemblies or 40 FAs for smaller fuel matrix [1]. The design of GBC-32 cask was directed by OECD/NEA concept, with the following criteria:

1. dimensions and geometry should be representative of typical U.S. rail type-casks;
2. the canister must accommodate at least 30 FAs;
3. the FA cell size must accommodate all common PWR designs;
4. design should be general without unique or proprietary information.

The GBC-32 design is based on merging OECD/NEA concepts with several U.S. cask vendors. Additional details on dimensions and materials of the cask can be found in report [1]. The reference fuel assembly design used in GBC-32 cask is the Westinghouse 17x17 Optimized Fuel Assembly (OFA) because it was shown to be the most reactive FA in most fresh-fuel cask designs. This fact streams from a zero burnup (fresh fuel) and high moderator-to-fuel ratio, which will at the same time produce less reactive fuel at typical discharge burnups. The OFA physical specification can be found in Table 1, while fresh fuel material specification for different fuel enrichments (2 w/o, 3 w/o, 4 w/o, and 5 w/o) can be found in report [1]. Figure 1 is showing NEWT 2D model of the OFA (green - fuel pins), which is placed inside GBC-32 cask cell.

Table 1

The OFA physical parameters

OFA parameter	inches	cm
Fuel outside diameter	0.3088	0.7844
Cladding inside diameter	0.3150	0.8001
Cladding outside diameter	0.3600	0.9144
Cladding radial thickness	0.0225	0.0572
Rod pitch	0.4960	1.2598
Guide tube inside diameter	0.4420	1.1227
Guide tube outside diameter	0.4740	1.2040
Guide tube radial thickness	0.0160	0.0406
Instrument tube inside diameter	0.4420	1.1227
Instrument tube outside diameter	0.4740	1.2040
Instrument tube radial thickness	0.0160	0.0406
Active fuel length	144	365.76
Array size	17x17	
Number of fuel rods	264	
Number of guide tubes	24	
Number of instrument tubes	1	

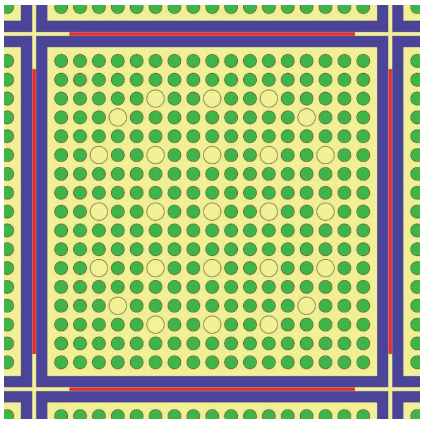

Fig. 1. Cross sectional view of OFA cell inside GBC-32 cask

III. Scale Computational Tools

The SCALE6.1.3 code system was developed for the U.S.NRC to satisfy a need for a standardized method of analysis for the evaluation of nuclear facilities and package designs. In its present form, the system has the capability to perform criticality, shielding, radiation source term, spent fuel depletion/decay, reactor physics, and sensitivity analyses using well established functional modules tailored to the SCALE6.1.3 system [3]. The TRITON sequence of the SCALE6.1.3 code system performs problem-dependent cross-section processing followed by calculation of neutron multiplication factor k-eff for a 2D FA configuration using NEWT. The NEWT module is a multigroup discrete-ordinates (SN) radiation transport code with flexible meshing capabilities that allows two-dimensional (2D) neutron transport calculations using complex geometric models. The differencing scheme employed by the NEWT, the Extended Step Characteristic approach (ESC), allows a computational mesh based on arbitrary polygons. This functionality can be iterated in tandem with ORIGEN-S depletion calculations to predict isotopic concentrations, source terms, and decay heat as a result of time-dependent fluxes calculated in a 2D deterministic fashion (NEWT) or in a 3D stochastic approach (KENO V.a or KENO-VI). Because spatial fluxes are burnup dependent, changing with nuclide inventories, and because mixture cross-sections will also change with burnup, the depletion sequence uses a predictor-corrector approach to update both fluxes and cross-sections as a function of burnup [4]. The rigorous SN treatment in NEWT coupled with ORIGEN-S depletion capabilities and CENTRM resonance self-shielding processing within TRITON sequence provides a high-fidelity approach for various FA designs. The cross-section processing can be CENTRM-based rigorous SN solution by default ("parm=centrm") or a more relaxed two-region approximation in CENTRM (similar in nature to NITAWL) but retaining continuous-energy processing ("parm=2region").

The main codes for this study thus simulate burnup/depletion (ORIGEN-S) and 2D neutron transport with eigenvalue search (NEWT) under TRITON. The ORIGEN-ARP code is used lastly to quantify isotopic source terms for different FA cooling periods. The use of this sequence requires availability of the cross-section libraries for a specific FA design. These may be obtained from pre-generated libraries distributed within SCALE6.1.3 or can be generated by the user for a specific FA design using true flux (not generic PWR) for cross-sections weighting.

A. TRITON-NEWT broad group library

The TRITON-NEWT parameter "weight" will trigger MALOCS module to generate a weighted broad group cross-section library in AMPX master format (newxnlib file). The calculated NEWT problem-averaged flux spectrum is then used as the weighting function for the spectral collapse, while user provides energy group structure in the "collapse" input block. For this analysis, the v7-238 group master library (148 fast + 90 thermal groups) based on ENDF/B-VII.0 [7] is collapsed to a user-defined 49-group library (v7-49g), with grouping structure tailored to important PWR flux peaks and windows. The distributed v5-44g library (based on ENDF/B-V) was developed to capture significant aspects of LWR spectrum, while newer 49-group structure introduced in SCALE6.0 includes additional energy groups in the upper thermal energy range.

B. ORIGEN-S cross section libraries

During TRITON depletion calculations, the module COUPLE is creating and updating a cross-section database (ft33f001 file) for each depleted material, thus providing cross-sections as a function

of burnup in specific ORIGEN-S file format. The TRITON produces one additional library with flux-weighted averaged cross-sections (ft33f001.cmbined file), which can be read by the ORIGEN-ARP module for rapid calculation of source terms. This procedure was adopted in this research for creating OFA libraries with different enrichment and burnup steps.

IV. Triton OFA Model

Based on the GBC-32 benchmark specification provided in Section 2, a computational model of the OFA was developed for TRITON-NEWT and TRITON depletion sequence. A cross sectional view of the NEWT 2D computational model is shown in Figure 2 for a symmetric 1/4 of the FA geometry. The calculations were performed using reasonably conservative cycle-average operational parameters for fuel temperature (1000 K), gap and clad temperature (620 K), moderator temperature (600 K), soluble boron concentration (650 ppm), and OFA specific power (40 MW/tU).

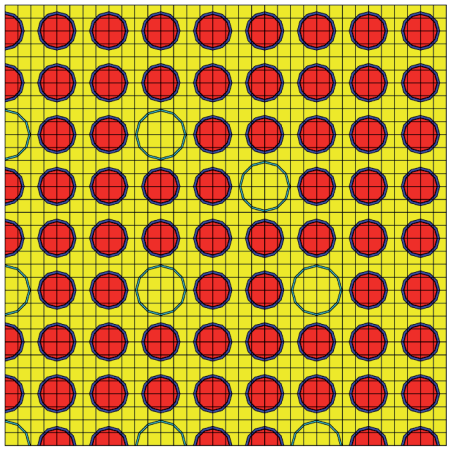

Fig. 2. NEWT model of the OFA with SN mesh (1/4 geometry)

The OFA fuel matrix is square 17x17 type (22.0 cm pitch) with 264 fuel rods and 24+1 control guide tubes. The fuel enrichment varies from 2 w/o to 5 w/o in ^{235}U using nominal thermal power of 40 MW/tU. The unit cell (1.2598 cm pitch) is comprised of fuel rod (1000 K), gap (620 K), clad (620 K) and moderator region (600 K) with 650 ppm of soluble boron. The cladding is Zirconium and the moderator is ordinary water. The NEWT model used S6 angular segmentation with P3 Legendre polynomial expansion for moderator (P1 for other materials), where unit cell had subdivision of 4x4 (recommended value). The forward transport solution was k-eff search with active collapse block (49 groups). The original coarse mesh finite difference (CMFD) acceleration was used for rectangular-domain configuration with enabled second-level two-group accelerator. All spatial and eigenvalue convergence criteria were set to value of $1 \cdot 10^{-4}$. The boundary conditions were all reflective type.

The TRITON depletion sequence was run using total of 20 time steps with duration of 75 days/step, giving total discharge burnup of 60 GWd/tU. The depletion with constant power was defined only for one material (UO_2 mixture, same for all pins) and three different libraries were used for k-eff comparison: v5-44g (broad built-in), v7-49g (user collapsed) and v7-238 (master built-in). The trace quantities of certain nuclides important for proper characterization of depleted fuel material were selected with "addnux=3" option, which adds 230 nuclides in depletion calculations.

The "parm=weight" option is very useful since TRITON depletion calculations require a significant amount of computer resources. This option allows generation of problem-dependent 49-group cross-section library at the start of depletion: steady-state NEWT calculation using v7-238 library is done only once at the beginning to determine neutron spectrum for spectral collapse. The 49-group library is then used for all subsequent depletion steps. This makes transport calculations run faster with minimal bias in total solution (typically less than 200 pcm for LWRs) [4]. Accurate depletion of heterogeneous FA designs in TRITON generally requires a different fuel mixture for every individual fuel pin inside a lattice, because spatial flux distribution varies significantly throughout a lattice model. Additionally, the flux distribution changes as a function of depletion. This results in space-time varying flux so fuel pin mixtures must be depleted individually in order to accurately track isotopic concentrations change [4]. Furthermore, depletion with a constant power is justified for fuel materials, but not for targets, structural materials and burnable poisons (i.e. IFBA rods). These materials are affected by neighboring fluxes and they do not contribute to power production, so depletion with a constant flux is a better option. Allowing mixed mode depletion with TRITON also improves the time-dependent flux distribution across fuel assembly.

V. Triton-NEWT OFA Results

The steady-state TRITON-NEWT results of k-eff are shown in Table 2 for different fuel enrichments using v7-238 master library (CPU time 11.5 min) and 49-group collapsed library (CPU time 2.1 min). One can notice small k-eff differences for v7-49g (40 pcm to 60 pcm) compared to v7-238 groups while CPU time reduction using broad library has almost linear scaling with the number of energy groups, i.e. v7-238 has over four times more groups than v7-49g. Figure 3 shows qualitatively neutron flux distribution over the 2D OFA model with e=2 w/o for the first and the last energy group. One can notice change in relative position of the local neutron sources from fuel rods (fast group) to water filled guide tubes (thermal group). The eigenvalue delta, or the change in k-eff with outer iterations is shown in Figure 4 using logarithmic scale to point out how final convergence will not be achieved until all group-wise inner iterations per outer iteration have converged.

Table II

NEWT steady-state k-eff solution

enrichment (w/o)	2.0	3.0	4.0	5.0
k-eff (v7-238)	1.11577	1.23911	1.31240	1.36101
k-eff (v7-49g)	1.11646	1.23977	1.31302	1.36158
k-eff rel.err. for v7-49g (pcm)	62.2737	53.7871	47.5313	41.9365

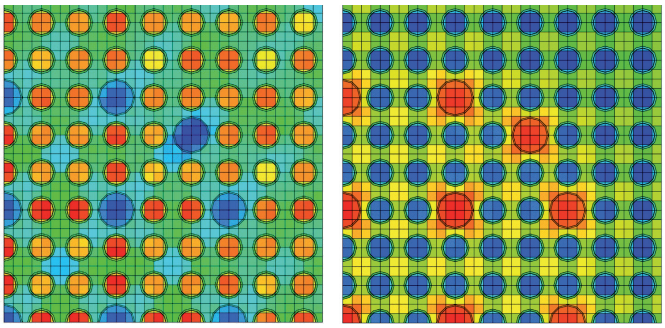

Fig. 3. NEWT flux distribution over OFA model (left-first group, right-last group)

Mario Matijević, Matej Pekeč, Characterization of the GBC-32 Fuel Assembly Source Terms, Journal of Energy, vol. 71 Number 4 (2022), 30–35
https://doi.org/10.37798/2022714467

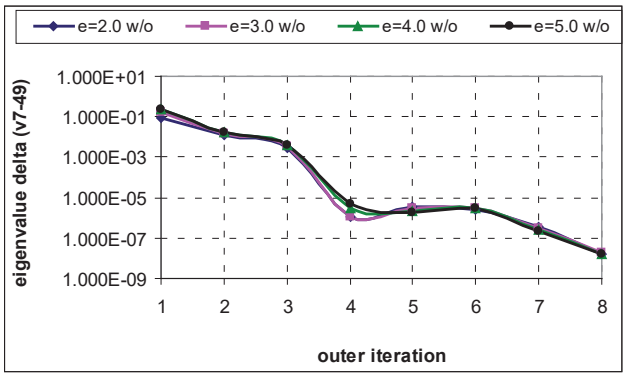

Fig.4. NEWT k-eff delta for v7-49g library

VI. Triton OFA depletion results

This section summarizes the depletion results for different enrichments of OFA model. Different cross-section libraries were used to investigate spectral effects on reactor physics parameters. The ENDF/B-VII.0 library v7-238 is generally recommended, but significantly prolongs CPU time per depletion step. Using a broad group library will automatically speed up the calculation, but the built-in v5-44g library (based on ENDF/B-V) was collapsed with LWR spectrum that is different than the specific OFA spectrum. This library is good for scoping and test calculations, but it is not recommended for production stage calculations. A good tradeoff between speed and accuracy can be obtained using the "parm=weight" option, which uses the problem-dependent neutron spectrum to collapse the master library v7-238 to a 49-group structure, which becomes working library for TRITON depletion sequence. The k-eff results for OFA (e=2.0 w/o) are shown in Figure 5, while v5-44g and v7-49g comparison to a master library v7-238 is shown in Figure 6. These trends are similar for other fuel enrichments and demonstrate justification of using collapsed v7-49g library for depletion calculations, reducing CPU run time by factor 4. One should also notice how delta k-eff for v7-49g library is bounded by an error interval of ± 100 pcm, which is a much smaller value compared to a built-in library v5-44g.

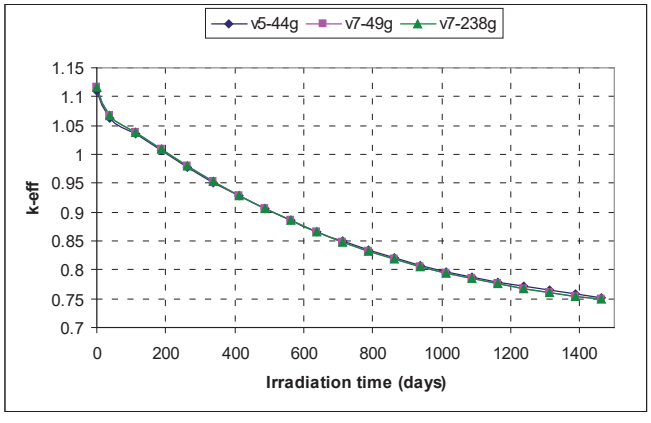

Fig. 5. TRITON k-eff depletion results (e=2.0 w/o)

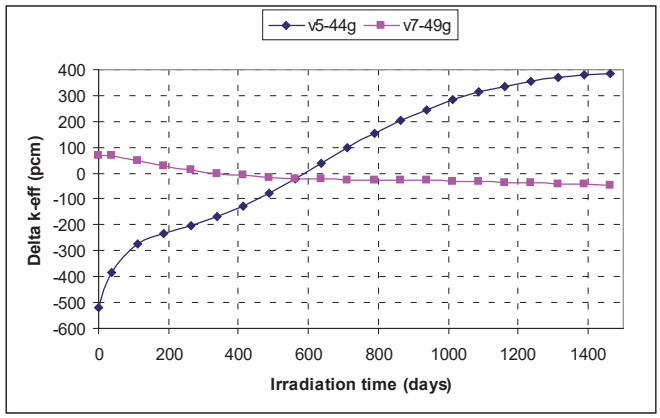

Fig. 6. Delta k-eff (pcm) for v5-44g and v7-49g libraries (e=2.0 w/o)

It is interesting to notice how delta k-eff curve of v5-44g library is being shifted to lower values for higher OFA enrichment levels, so Figure 7 is presenting this trend for e=5.0 w/o.

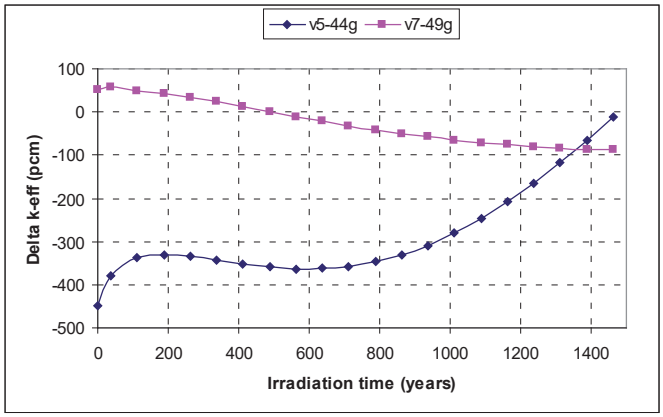

Fig. 7. Delta k-eff (pcm) for v5-44g and v7-49g libraries (e=5.0 w/o)

Relative pin power distribution of the OFA model is shown in Figure 8 for the fresh fuel (left) and at the end of irradiation (right). The peak pin power of 1.0655 was in the fuel rod (5, 6) for the fresh fuel and 1.0646 in the same position for burnt fuel, respectively.

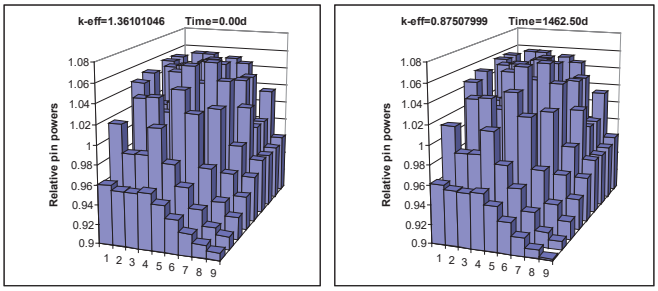

Fig. 8. Relative pin power distribution in the OFA (e=5.0 w/o)

Another useful result obtained with TRITON depletion is generation of ORIGEN-S cross-section libraries for depleted material. These burnup-dependent libraries were appended to SCALE6.1.3 data directory so ORIGEN-ARP module could be used for a rapid calculation of OFA source terms. The ORIGEN-ARP results are presented next using PlotOPUS program [3] for v7-27n19g shielding library, burnup of 60 GWd/tU, specific power of 40 MW/tU, 3 burnup cycles, and cooling periods of 0, 1, 3, 10, 30, and 40 years. The multigroup gamma and neutron spectra are shown in Figure 9 and Figure 10, while Figure 11 shows primary contributors (light elements, actinides and fission products) for decay heat production in order of their importance, but total value is for all nuclides in the

Mario Matijević, Matej Pekeč, Characterization of the GBC-32 Fuel Assembly Source Terms, Journal of Energy, vol. 71 Number 4 (2022), 30–35
https://doi.org/10.37798/2022714467

problem. The multigroup neutron and gamma sources (particles/s/tU) are depicted in Figure 12 and Figure 13 for e=2.0 w/o, while total n-g sources as a function of cooling time are depicted in Figures 14 and 15, showing characteristic falling-off trend.

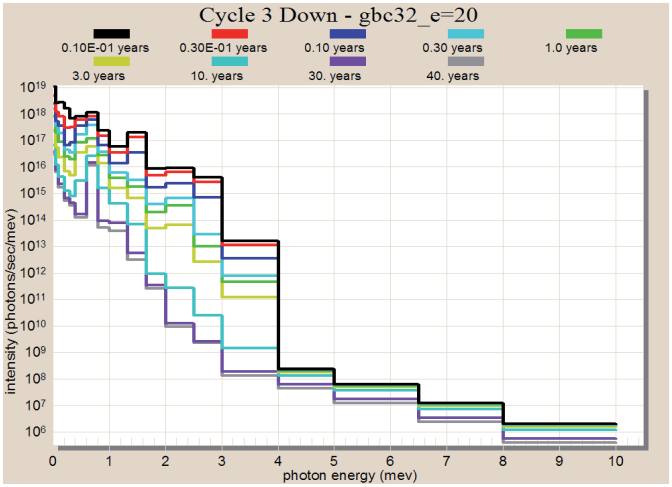

Fig. 9. Gamma spectra in photons/s/MeV (e=2.0 w/o)

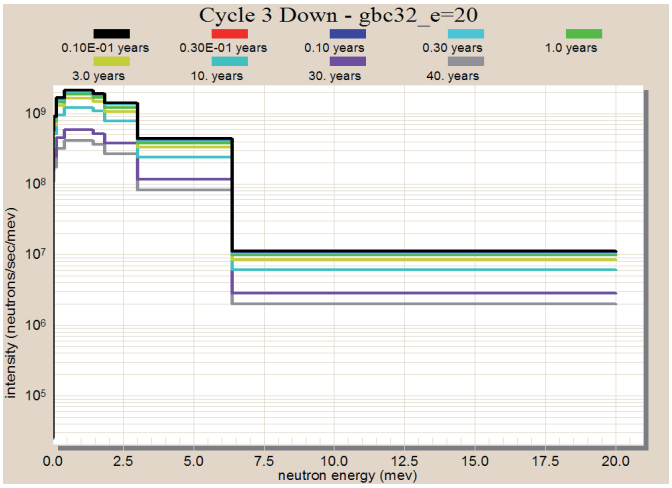

Fig. 10. Total neutron spectra in neutrons/s/MeV (e=2.0 w/o)

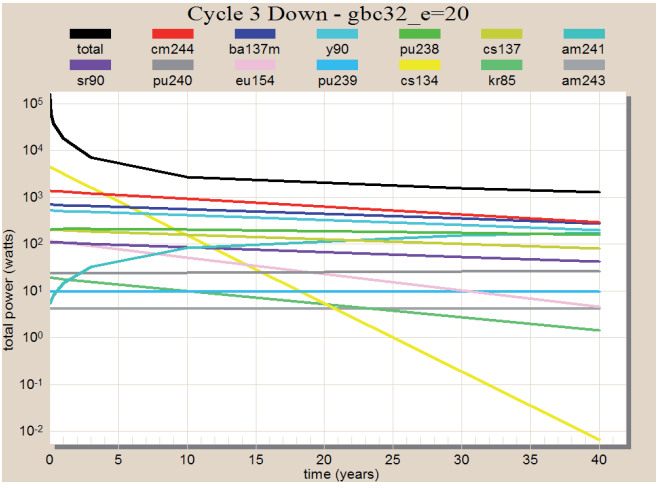

Fig. 11. Decay heat primary contributors (e=2.0 w/o)

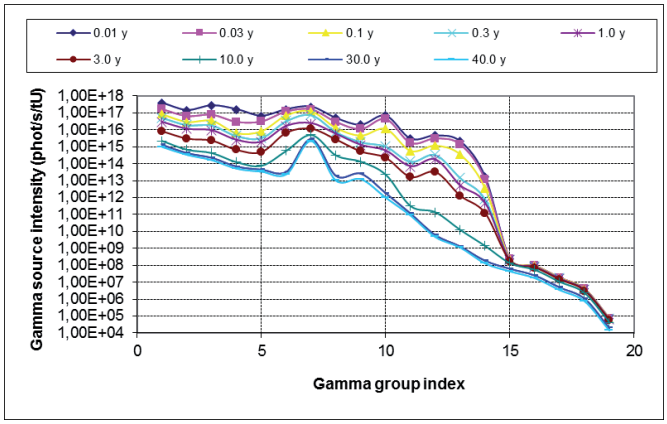

Fig. 12. Gamma source intensity (phot/s/tU) for different groups (e=2.0 w/o)

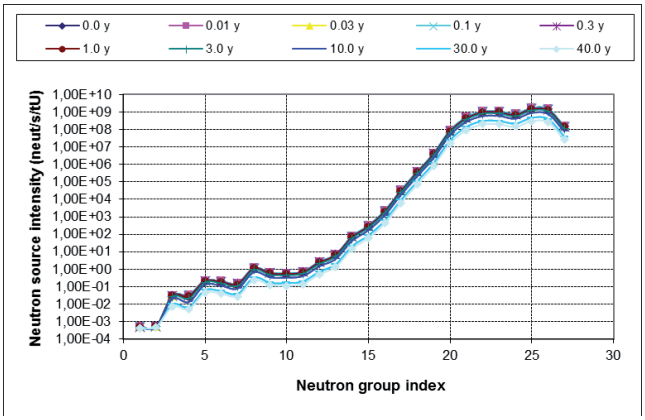

Fig. 13. Neutron source intensity (neut/s/tU) for different groups (e=2.0 w/o)

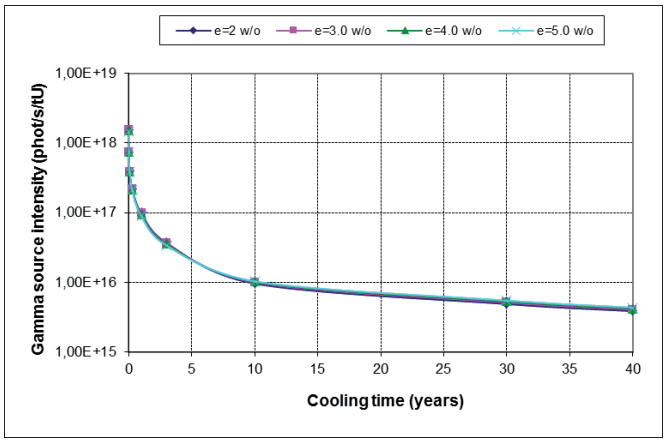

Fig. 14. Gamma source intensity (phot/s/tU) as a function of cooling time

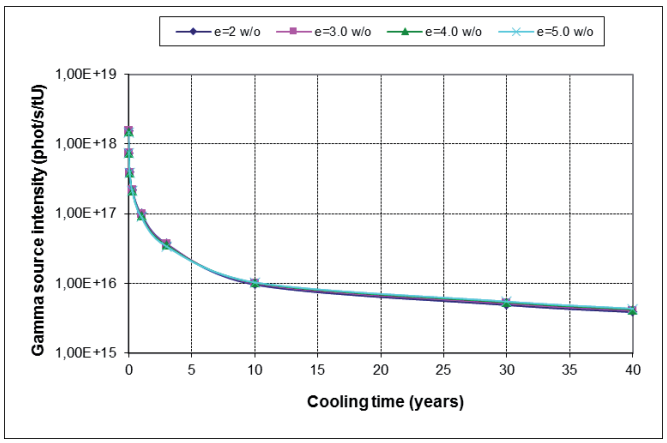

Fig. 15. Neutron source intensity (neut/s/tU) as a function of cooling time

Mario Matijević, Matej Pekeč, Characterization of the GBC-32 Fuel Assembly Source Terms, Journal of Energy, vol. 71 Number 4 (2022), 30–35
https://doi.org/10.37798/2022714467

VII. Discussion and Conclusions

This paper presents selected results of TRITON-NEWT and TRITON depletion simulations of the OFA model in the framework of GBC-32 cask benchmark. This first phase is addressing accurate source terms characterization, since OFA model contains small modifications compared to the standard Westinghouse 17x17 FA model. Besides quantification of neutron-gamma source terms, during burnup and cooling time periods, this methodology provides ability to generate cross-section database (ft33f001 file) for each depleted material as a function of burnup in ORIGEN-S format. Such approach will use the initial v7-238 NEWT flux solution of the OFA model as a weighting function in production of the v7-49g collapsed cross-section library, which will accelerate remaining TRITON depletion calculations with a minimal bias in a solution. The obtained time-dependent databases can be directly used with ORIGEN-ARP interpolator to produce comprehensive source term characterization. The obtained results will be used in preparation of specific neutron-gamma source terms for the future MAVRIC/Monaco shielding calculations of GBC-32 cask.

The presented calculations utilize symmetry of the OFA model, so only 1/4 of FA was modeled with reflective boundary conditions. On top of that, each fuel pin had the same UO_2 matrix as the only depleted material, which is a gross approximation for modern FA designs. In practice, considerable CPU time goes on cross-section processing (CENTRM module) prior to NEWT calculations if one chooses to deplete a large number of fuel mixtures [8]. Moreover, this CPU time becomes prohibitively large with multiple unit cells, which are necessary for capturing spatial effects of fuel depletion. This problem is a well-known issue in depletion of modern, heterogeneous FA designs, that even with symmetry inclusion one typically gets dozens of fuel pin locations which need to be independently depleted. To simplify cross-section processing paradigm, it has been recognized that the macroscopic response of spent fuel is much more sensitive to the number densities of constituent nuclides than the nuclide cross-sections [3][4].

References

[1] "Computational Benchmark for Estimation of Reactivity Margin from Fission Products and Minor Actinides in PWR Burnup Credit", Prepared by J. C. Wagner, NUREG/CR-6747, ORNL/TM-2000/306.

[2] "Standard Review Plan for Dry Cask Storage Systems", NUREG-1536, U.S. NRC, Washington, D.C., January 1997.

[3] "SCALE: A Comprehensive Modeling and Simulation Suite for Nuclear Safety Analysis and Design", ORNL/TM-2005/39, Version 6.1, June 2011. Available from Radiation Safety Information Computational Center at Oak Ridge National Laboratory as CCC-785.

[4] "SCALE/TRITON Primer: A Primer for Light Water Reactor Lattice Physics Calculations", NUREG/CR-7041, ORNL/TM-2011/21, Oak Ridge National Laboratory 2012.

[5] E. E. Lewis, W. F. Jr. Miller, "Computational Methods of Neutron Transport", American Nuclear Society, Illinois, 1993.

[6] "OrigenArp Primer: How to Perform Isotopic Depletion and Decay Calculations with SCALE/ORIGEN", prepared by S. M. Bowman, I. C. Gauld, ORNL/TM-2010/43.

[7] M.B. Chadwick, et al, "ENDF/B-VII.0: Next Generation Evaluated Nuclear Data Library for Nuclear Science and Technology", Nuclear Data Sheets, 107, 12, pp. 2931-3060, (2006).

[8] R. Ječmenica, M. Matijević, D. Grgić, "Fuel Depletion Modeling of Reconstituted NEK Fuel Assembly Using Lattice Cell Programs", Proceedings of the 10th International Conference on Nuclear Option in Countries with Small and Medium Electricity Grids, Zadar, Croatia, 1-4 June 2014, pp. 154.1 – 154.13.

ENERGIJA